

See discussions, stats, and author profiles for this publication at: <https://www.researchgate.net/publication/231525272>

Solvated silylium cations: structure determination by NMR spectroscopy and the NMR/Ab initio/IGLO method. J Am Chem Soc

ARTICLE *in* JOURNAL OF THE AMERICAN CHEMICAL SOCIETY · MAY 1996

Impact Factor: 12.11 · DOI: 10.1021/ja9542956

CITATIONS

56

READS

18

5 AUTHORS, INCLUDING:



Dan Johnels

Umeå University

60 PUBLICATIONS 843 CITATIONS

SEE PROFILE



U. G. Edlund

140 PUBLICATIONS 2,818 CITATIONS

SEE PROFILE

Solvated Silylium Cations: Structure Determination by NMR Spectroscopy and the NMR/Ab Initio/IGLO Method

Mehrdad Arshadi,[†] Dan Johnels,[†] Ulf Edlund,^{*,†} Carl-Henrik Ottosson,[‡] and Dieter Cremer^{*,‡}

Contribution from the Department of Organic Chemistry, Umeå University, S-901 87 Umeå, Sweden, and Department of Theoretical Chemistry, Göteborg University, Kemigården 3, S-412 96 Göteborg, Sweden

Received December 28, 1995[®]

Abstract: Sixty R_3SiX /solvent (S) and R_2HSiX/S systems with R = methyl, ethyl, butyl and S = methylene chloride, DMPU, DMSO, sulfolane, HMPA, acetonitrile, pyridine, N -methylimidazole, and triethylamine were investigated with the help of NMR spectroscopy for different concentration ratios of R_3SiX/S and R_2HSiX/S as well as different temperatures. With the help of measured $\delta^{29}Si$ and $\delta^{13}C$ chemical shifts as well as $^1J_{Si-C}$ and $^2J_{Si-P}$ coupling constants, typical NMR parameters for R_3SiX and R_2HSiX , $R_3Si(S)^+$, $R_2HSi(S)^+$, and $R_2HSi(S)_2^+$ were established and discussed to distinguish between possible silylium cation–solvent complexes and equilibria between them. In addition, the NMR/ab initio/IGLO method (based on the continuum solvent model PISA and IGLO-PISA chemical shift calculations) was used to determine geometry, stability, and other properties of $Me_3Si(S)_n^+$ and $Me_2HSi(S)_n^+$ complexes in different solutions. NMR measurements and ab initio calculations clearly show that $R_3Si(S)^+$ and $R_2HSi(S)^+$ complexes with tetracoordinated Si are formed with solvents (S) more nucleophilic than methylene chloride while complexes with two S molecules and a pentacoordinated Si atom can only be found for $R_{3-n}H_nSi^+$ cations with $n \geq 1$. This is a result of internal (hyperconjugative) stabilization of R_3Si^+ by alkyl groups and external stabilization by S coordination, as well as of steric factors involving R and S. Complex binding energies are in the range of 40–60 kcal/mol, which is significantly different from complex binding energies in the gas phase. In all cases investigated, (weakly) covalent bonds between Si and S are formed that exclude any silylium cation character for the solvated R_3Si^+ and R_2HSi^+ ions.

1. Introduction

Reactions involving silicon-containing reagents are of importance for synthetic organic chemistry, where for instance silyl hydrides can be used for selective reductions of alkenes.^{1–3} The central step in such reduction processes can be formulated as a hydride transfer from a silane to a carbocation, involving the formation of a silicon cationic species.³ Furthermore, trimethylsilyl iodide⁴ and trimethylsilyl triflate⁵ are widely used reagents and their usage for instance in cleavage reactions of esters and ethers presumably involves ionic reaction intermediates.

Enhanced interest in silylium cations R_3Si^+ ⁶ also exists because of the ongoing debate on the degree of complexation

of R_3Si^+ cations in solution.^{7–13} Lambert and co-workers published several reports on the proposed formation of nearly free R_3Si^+ ions in condensed phases.⁸ Their claims were criticized by a number of authors including Olah, Cremer, Schleyer, Pauling, and others.^{9–12} Based on 1H , ^{13}C , $^{35/37}Cl$, ^{15}N , and ^{19}F NMR spectroscopy, cryostatic and X-ray crystal-

(8) (a) Lambert, J. B.; Schulz, W. J. *J. Am. Chem. Soc.* **1983**, *105*, 1671. (b) Lambert, J. B.; McConnell, J. A.; Schulz, W. J. *J. Am. Chem. Soc.* **1986**, *108*, 2482. (c) Lambert, J. B.; Schilf, W. *J. Am. Chem. Soc.* **1988**, *110*, 6364. (d) Lambert, J. B.; Schulz, W. J.; McConnell, J. A.; Schilf, W. *J. Am. Chem. Soc.* **1988**, *110*, 2201. (e) Lambert, J. B.; Kania, L.; Schilf, W.; McConnell, J. A. *Organometallics* **1991**, *10*, 2578. (f) Lambert, J. B.; Zhang, S. *J. Chem. Soc., Chem. Commun.* **1993**, 383. (g) Lambert, J. B.; Zhang, S.; Stern, C. L.; Huffman, J. C. *Science* **1993**, *260*, 1917. (h) Lambert, J. B.; Zhang, S.; Ciro, S. M. *Organometallics* **1994**, *13*, 2430. (i) Lambert, J. B.; Zhang, S. *Science*, **1994**, *263*, 984.

(9) (a) Olah, G. A.; Heiliger, L.; Li, X. Y.; Prakash, G. K. S. *J. Am. Chem. Soc.* **1990**, *112*, 5991. (b) Prakash, G. K. S.; Keyaniyan, S.; Aniszfeld, R.; Heiliger, L.; Olah, G. A.; Stevens, R. C.; Choi, H. K.; Bau, R. *J. Am. Chem. Soc.* **1987**, *109*, 5123. (c) Olah, G. A.; Rasul, G.; Heiliger, L.; Bausch, J.; Prakash, G. K. S. *J. Am. Chem. Soc.* **1992**, *114*, 7737. (d) Olah, G. A.; Rasul, G.; Li, X.; Buchholz, H. A.; Sandford, G.; Prakash, G. K. S. *Science*, **1994**, *263*, 983. (e) Olah, G. A.; Rasul, G.; Buchholz, H. A.; Li, X.-Y.; Prakash, G. K. S. *Bull. Soc. Chim. Fr.* **1995**, *132*, 569. (f) Olah, G. A.; Li, X.-Y.; Rasul, G.; Prakash, G. K. S. *J. Am. Chem. Soc.* **1995**, *117*, 8962.

(10) (a) Olsson, L.; Ottosson, C.-H.; Cremer, D. *J. Am. Chem. Soc.* **1995**, *117*, 7460. (b) Olsson, L.; Cremer, D. *Chem. Phys. Lett.* **1993**, *215*, 433.

(11) (a) Schleyer, P. v. R.; Buzek, P.; Müller, T.; Apeloig, Y.; Siehl, H.-U. *Angew. Chem.* **1993**, *105*, 1558. (b) Mearker, C.; Kapp, J.; Schleyer, P. v. R. *Organosilicon Chemistry*; Auner, N., Weis, J., Eds.; VCH (Weinheim): Weinheim, Germany, 1996; Vol. II, p 329.

(12) Pauling, L. *Science* **1994**, *263*, 983.

(13) (a) Reed, C. A.; Xie, Z. *Science*, **1994**, *263*, 985. (b) Xie, Z.; Bau, R.; Reed, C. A. *J. Chem. Soc., Chem. Commun.* **1994**, 2519. (c) Reed, C. A.; Xie, Z.; Bau, R.; Benesi, A. *Science* **1993**, *262*, 402. (d) Xie, Z.; Liston, D. J.; Jelinek, T.; Mitro, V.; Bau, R.; Reed, C. A. *J. Chem. Soc., Chem. Commun.* **1993**, 384. (e) Xie, Z.; Bau, R.; Benesi, A.; Reed, C. A. *Organometallics* **1995**, *14*, 3933.

[†] Umeå University.

[‡] Göteborg University.

[®] Abstract published in *Advance ACS Abstracts*, May 1, 1996.

(1) Weber, W. P. *Silicon Reagents for Organic Synthesis*; Springer-Verlag: New York, 1983; p 273.

(2) (a) Larson, G. L. In *The Chemistry of Organosilicon Compounds*; Patai, S., Rappoport, Z., Eds.; Wiley Interscience: New York, 1989; p 763.

(3) Fleming, I. *Organic Silicon Chemistry in Comprehensive Organic Chemistry*; Barton, O.; Ollis, W. D., Eds.; Pergamon Press: New York, 1979; Vol. 3, p 541.

(4) (a) Olah, G. A.; Prakash, G. K. S.; Krishnamurti, R. *Adv. Silicon Chem.* **1991**, *1*, 1.

(5) (a) Emde, H.; Domsch, D.; Feger, H.; Frick, U.; Götz, A.; Hergott, H. H.; Hofmann, K.; Kober, W.; Krägeloh, K.; Oesterle, T.; Steppen, W.; West, W.; Simchen, G. *Synthesis* **1982**, 1.

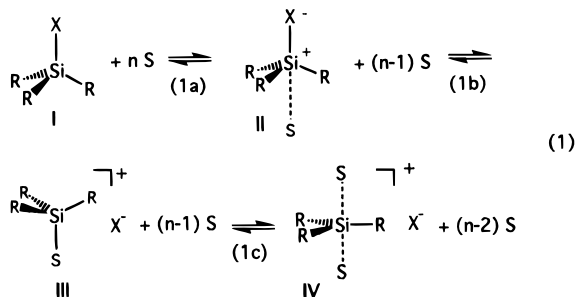
(6) We use the term silylium cation for R_3Si^+ rather than silicenium ion, silylenium ion, or silyl cation, thus following recent IUPAC recommendations. See: *Nomenclature of Inorganic Chemistry*; Leigh, G. J., Ed.; Blackwell: Oxford, U.K., 1990; p 106.

(7) For recent reviews on the work on R_3Si^+ in solution see: (a) Lambert, J. B.; Kania, L.; Zhang, S. *Chem. Rev.* **1995**, *95*, 1191. (b) Chojnowski, J.; Stanczyk W.; *Adv. Organomet. Chem.* **1990**, *30*, 243. (c) Chojnowski, J.; Stanczyk W.; *Main Group Chem. News* **1994**, *2*, 6. (d) Lickiss, P. D. *J. Chem. Soc., Dalton Trans.* **1992**, 1333.

lographic measurements, and ab initio calculations, it was shown that in none of the cases reported in the literature were truly uncoordinated silylium ions generated in solution.^{9–12}

There is compelling evidence indicating that the silylium cations generated by Lambert and co-workers in solution correspond to Wheland σ -complexes, which have largely lost any silylium cation character. Clearly, the free silylium cation in solution is a fiction, and the issue is not whether one can generate it, but how much silylium cation character (if any at all) can be retained in a solvent (S)-coordinated silylium cation. As solvent coordination becomes weaker, the properties of a totally free silylium cation in solution may be extrapolated and the question of how R_3Si^+ can become S-independent in solution can be answered.

In view of the present interest in solvated silylium cations and their role as reaction intermediates, it is desirable to determine the degree of complexation of R_3Si^+ by S molecules in solution. S complexation could occur as described by reactions 1a, 1b, and 1c, in which first pentacoordinated silane **II**, then a tetracoordinated silyl cation **III**, and finally pentacoordinated siliconium ion **IV** are formed. As was shown in a recent ab initio investigation,^{10a} additional S molecules can group around the silyl cation; however, these molecules are less tightly bound as is reflected by calculated Si–S distances and com-



plexation energies. One can speak of a first “solvent shell” containing maximally two S molecules and a second solvent shell with up to 12 molecules.^{10a} Alternatively, one can consider **II**, **III**, and **IV** as new well-defined silicon compounds that in solution are surrounded by a solvent shell. The following discussion will show that the later description is more reasonable.

Although the complexation process sketched by reaction 1 represents a simplification, which does not distinguish between the formation of contact ion pairs, solvent-separated ion pairs, etc. and does not consider the structure of the solvent shell, this representation is rather useful when describing the most important steps of silylium cation interactions with the solvent. In particular, process 1 makes it clear that each solvation step can be reversible so that reaction equilibria between **I**, **II**, **III**, and **IV** have to be considered, which complicates experimental investigations so far as temperature and/or concentration studies need to be carried out.

In the literature, there are already numerous descriptions of R_3SiX in many different solvents where in particular the work by Bassindale, Stout, and co-workers has to be mentioned.^{14–17} These researchers found that upfield shifts in the $\delta^{29}\text{Si}$ values result when monoalkylsilyl triflates (RH_2SiOTf) are solved in CH_2Cl_2 together with the nucleophilic solvents N,N' -dimethyl-

propyleneurea (DMPU) or hexamethylphosphortriamide (HMPA).¹⁴ Conductivity was not observed at equal concentrations of nucleophilic solvent S and silyl triflate, which suggests the formation of a neutral pentacoordinated Si complex of type **II**. Such a complex was also formed between H_3SiCl and dimethyl ether in the solid state.¹⁸ When more solvent was added to the silyl triflate solution, the conductivity increased sharply in line with formation of cationic complexes **III** and/or **IV**.

On the other hand, trimethylsilyl triflate, Me_3SiOTf , directly forms conducting solutions in nucleophilic solvents S.¹⁵ For systems where the equilibrium is in favor of a tetracoordinated type **III** salt $[\text{Me}_3\text{Si}(\text{S})]^+\text{OTf}^-$, changes in the $\delta^{29}\text{Si}$ values were not observed when going from trimethylsilyl triflate to the corresponding iodide. Conductometric titration measurements also gave proof for the formation of a type **III** complex. Dimethylsilyl triflate showed interesting behavior in ^{29}Si shift titrations with either *N*-methylimidazole (NMI) or pyridine.^{16b} Two ^{29}Si signals centered at 24 and 10 ppm appear at ratios of NMI:silyl triflate lower than 1:1. The first of these signals corresponds to the original silyl triflate, while the second is ascribed to a tetracoordinated Si salt of type **III**. With an excess of NMI, a change in $\delta^{29}\text{Si}$ was observed approaching a limiting value of -82 ppm, which was considered to originate from a pentacoordinated Si complex of type **IV**.

Kira, Sakurai, and co-workers showed that Me_3Si^+ generated from trimethylsilyl tetrakis[3,5-bis(trifluoromethyl)phenyl]borate (Me_3SiTfPB) in CD_2Cl_2 together with diethyl ether exists as a stable tetracoordinated silyloxonium ion $\text{Me}_3\text{Si}(\text{OEt}_2)^+$.¹⁹ Attempted generation of silylium ions in pure CD_2Cl_2 did not succeed since only signals due to trimethylsilyl chloride and fluoride were detected. Furthermore, solvation of silyl hydrides in CD_2Cl_2 with added amounts of acetonitrile results in formation of silylnitrilium ions $\text{R}_3\text{Si}(\text{NCR}')^+$ with tetracoordinated Si.²⁰ Hensen and co-workers determined the X-ray crystal structure of $[\text{Me}_3\text{Si}(\text{pyridine})]^+\text{I}^-$, which showed that the Si atom is tetravalent but slightly perturbed toward trivalency.²¹ These authors also determined the crystal structure of $\text{Me}_2\text{HSi}(\text{NMI})_2^+$, which reveals that Si is pentacoordinated in the solid state.²² Ab initio investigations performed by Cremer and co-workers on SiH_3^+ and Me_3Si^+ coordinated by solvent prototypes reveal that S coordination to R_3Si^+ can lead to complexation energies larger than 100 kcal/mol and that ^{29}Si signals are upfield shifted to as much as -130 ppm.^{10a}

Information on complexation energies between R_3Si^+ and Lewis bases S in the gas phase is also available from mass spectrometry investigations.^{23–26} The largest $\text{Me}_3\text{Si}(\text{S})^+$ complexation energies are found for amines (40–60 kcal/mol).²⁴ It was shown that the complex binding energies increase with the

(18)) Blake, A. J.; Craddock, S.; Ebsworth, E. A. V.; Franklin, K. C. *Angew. Chem., Int. Ed. Engl.* **1990**, 29, 76.

(19)) Kira, M.; Hino, T.; Sakurai, H. *J. Am. Chem. Soc.* **1992**, 114, 6697.

(20)) (a) Kira, M.; Hino, T.; Sakurai, H. *Chem. Lett.* **1993**, 153. (b) Bahr, S.; Boudjouk, P. *J. Am. Chem. Soc.* **1993**, 115, 4514.

(21)) Hensen, K.; Zengerly, T.; Pickel, P.; Klebe, G. *Angew. Chem.* **1983**, 95, 739.

(22)) Hensen, K.; Zengerly, T.; Müller, T.; Pickel, P. *Z. Anorg. Allg. Chem.* **1988**, 558, 21.

(23)) For a review on R_3Si^+ in the gas phase see: Schwarz, H. In *The Chemistry of Organic Silicon Compounds*, Patai, S., Rappoport, Z., Eds.; Wiley Interscience: New York, 1989; p 445.

(24)) Li, X.; Stone, J. A. *Int. J. Mass Spectrom. Ion Processes* **1990**, 101, 149.

(25)) (a) Wojnytiak, A. C. M.; Stone, J. A. *Int. J. Mass Spectrom. Ion Processes* **1986**, 74, 59. (b) Stone, J. A.; Wojnytiak, A. C. M.; Wytenburg, W. *Can. J. Chem.* **1986**, 64, 575.

(26)) (a) Cacace, F.; Crestoni, M. A.; Fornarini, S. *Int. J. Mass Spectrom. Ion Processes* **1988**, 84, 17. (b) Stone, J. M.; Stone, J. A. *Int. J. Mass Spectrom. Ion Processes* **1991**, 109, 247. (c) Cacace, F.; Attina, M.; Fornarini, S. *Angew. Chem.* **1995**, 107, 754.

(14)) (a) Bassindale, A. R.; Jiang, J. J. *Organomet. Chem.* **1993**, 446, C3. (b) Bassindale, A. R.; Stout, T. J. *Organomet. Chem.* **1984**, 271, C1.

(15)) Bassindale, A. R.; Stout, T. *Tetrahedron Lett.* **1985**, 26, 3403.

(16)) (a) Bassindale, A. R.; Stout, T. J. *Chem. Soc., Perkin Trans. 2* **1986**, 221. (b) Bassindale, A. R.; Stout, T. J. *Chem. Soc., Chem. Commun.* **1984**, 1387.

(17)) Bassindale, A. R.; Stout, T. J. *Organomet. Chem.* **1982**, 238, C41.

donicity of S; however, steric effects can lead to reduction of the binding energies.²⁴

It has been claimed that trimethylsilyl compounds Me_3SiX either react to a cationic species $\text{R}_3\text{Si}(\text{S})^+$ or do not react at all.¹⁷ This is in line with a statement of Chuit, Corriu, Reye, and Young that "complexes in which the coordination at silicon is increased to five (or six) are formed only when there is more than one electronegative ligand bonded to the parent organo-silicon compound or when hydrogen is a ligand as well".²⁷

Despite the fact that a large number of investigations has been performed to describe the fate of R_3SiX in solution, many questions on the degree of complexation, the resulting electronic structure changes in R_3Si^+ , and the remaining silylium cation character of R_3Si^+ are still unanswered. In this work, we report results of a two-pronged approach that combines NMR measurements of silylium cations in solution and the ab initio calculation of the very same ions. Central to our approach is the NMR/ab initio/individual gauge for localized orbitals (IGLO) method which provides an excellent tool for determining geometry and other properties of solvated molecules by NMR spectroscopy.^{28,29} This method is based on the sensitivity of NMR chemical shifts with regard to the degree of complexation and in particular geometrical distortions caused by solvent complexation of the target molecule. Only if these factors are adequately described by theory can experimental shifts be reproduced. However, if experimental and calculated NMR chemical shifts agree within the given accuracy of the ab initio method used, then the geometry of the ab initio structure will be a good model of the target system in solution.^{28,29}

In this work, we will use (a) NMR measurements carried out on 60 different $\text{R}_3\text{SiX/S}$ and $\text{R}_2\text{HSiX/S}$ systems, where R, X, and S are varied and changes in concentration and temperature are made, and (b) the NMR/ab initio/IGLO method to discuss questions that concern the mechanism of solvation (see 1 below), the stability of $\text{R}_3\text{Si}(\text{S})_n^+$ ($n = 1$ or 2) complexes (see 2 below), their geometry and other properties (see 3 and 4 below), the type of interaction between S and R_3Si^+ (electrostatic or covalent (see 5 below)), and the silylium character of $\text{R}_3\text{Si}(\text{S})_n^+$:

(1) Under what conditions can the formation of tetracoordinated Si complexes $\text{R}_3\text{Si}(\text{S})^+$ and $\text{R}_2\text{HSi}(\text{S})^+$ (type **III**) or pentacoordinated Si complexes $\text{R}_3\text{Si}(\text{S})_2^+$ and $\text{R}_2\text{HSi}(\text{S})_2^+$ (type **IV**) be expected?

(2) How stable are complexes $\text{R}_3\text{Si}(\text{S})_n^+$ and $\text{R}_2\text{HSi}(\text{S})_n^+$? How does the stability depend on substituents R and the nucleophilic character of solvent S?

(3) What is the geometry of ions $\text{R}_3\text{Si}(\text{S})_n^+$ and $\text{R}_2\text{HSi}(\text{S})_n^+$ in solution? Does the geometry of the $\text{R}_3\text{Si}^+/\text{R}_2\text{HSi}^+$ part of the complex change with regard to its gas-phase geometry?

(27)) Chuit, C.; Corriu, R. J. P.; Reye, C.; Young, J. C. *Chem. Rev.* **1993**, 93, 1371.

(28)) (a) Cremer, D.; Olsson, L.; Reichel, F.; Kraka, E. *Isr. J. Chem.* **1993**, 33, 369. (b) Cremer, D.; Reichel, F.; Kraka, E. *J. Am. Chem. Soc.* **1991**, 113, 9459. (c) Svensson, P.; Reichel, F.; Ahlberg, P.; Cremer, D. *J. Chem. Soc., Perkin Trans. 2* **1991**, 1463. (d) Cremer, D.; Svensson, P.; Kraka, E.; Ahlberg, P. *J. Am. Chem. Soc.* **1993**, 115, 7445. (e) Sieber, S.; Schleyer, P. v. R.; Otto, A. H.; Gauss, J.; Reichel, F.; Cremer, D. *J. Phys. Org. Chem.* **1993**, 6, 445. (f) Szabo, K.; Kraka, E.; Cremer, D. *J. Org. Chem.* To be published.

(29)) See, e.g.: (a) Hnyk, D.; Vajda, E.; Buehl, M.; Schleyer, P. v. R. *Inorg. Chem.* **1992**, 31, 2464. (b) Buehl, M.; Schleyer, P. v. R. *J. Am. Chem. Soc.* **1992**, 114, 477. (c) Buehl, M.; Schleyer, P. v. R.; McKee, M. L. *Heteroat. Chem.* **1991**, 2, 499. (d) Buehl, M.; Schleyer, P. v. R. *Angew. Chem.* **1990**, 102, 962. (e) Schleyer, P. v. R.; Buehl, M.; Fleischer, U.; Koch, W. *Inorg. Chem.* **1990**, 29, 153. (f) Schleyer, P. v. R.; Koch, W.; Liu, B.; Fleischer, U. *J. Chem. Soc., Chem. Commun.* **1989**, 1098. (g) Bremer, M.; Schoetz, K.; Schleyer, P. v. R.; Fleischer, U.; Schindler, M.; Kutzelnigg, W.; Koch, W.; Pulay, P. *Angew. Chem.* **1989**, 101, 1063. (h) Bühl, M.; Steinke, T.; Schleyer, P. v. R.; Boese, R. *Angew. Chem., Int. Ed. Engl.* **1991**, 30, 1160.

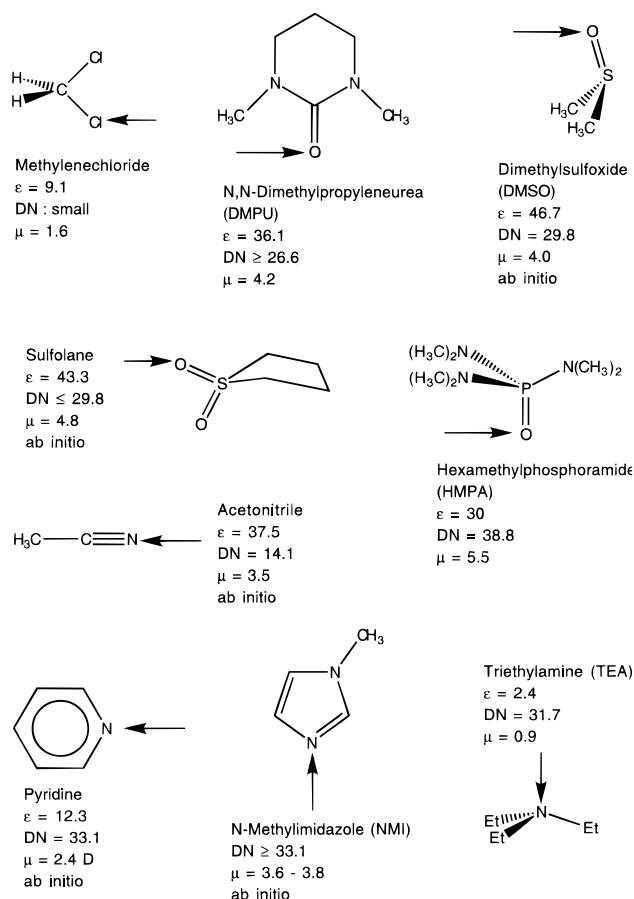


Figure 1. Structures, dielectricity constants, donicities, and dipole moments of solvents used. Donicities (DN) are given in kcal/mol,^{31a} and dipole moments (μ) in Debye.^{31b,c} Solvents used in the theoretical part of the paper are labeled with the term "ab initio". The coordinating atoms in the solvents are marked with arrows.

(4) Are there differences in the electronic and magnetic properties of $\text{R}_3\text{Si}(\text{S})_n^+/\text{R}_2\text{HSi}(\text{S})_n^+$ in solution and $\text{R}_3\text{Si}^+/\text{R}_2\text{HSi}^+$ or $\text{R}_3\text{Si}(\text{S})_n^+/\text{R}_2\text{HSi}(\text{S})_n^+$ in the gas phase?

(5) Are $\text{R}_3\text{Si}^+/\text{R}_2\text{HSi}^+$ and S bonded by electrostatic or covalent interactions? How do the interactions between the complex partners change with R and S?

(6) To what extent do complexes $\text{R}_3\text{Si}(\text{S})_n^+$ still represent silylium ions and how S independent are these cations? In other words, can one speak in any case of nearly free (weakly S complexed) silylium cations?

In the following we will present the results of this investigation by first describing results of the NMR measurements and, then, discussing the results of the NMR/ab initio/IGLO investigation.

2. NMR Investigation

The behavior of silanes R_3SiX and R_2HSiX was investigated in solvents ranging from the weakly donating NCCD_3 and sulfolane to the strongly donating HMPA and dimethyl sulfoxide (DMSO). The effects of counterions were studied along the line of decreasing coordinating ability in the series Cl^- , OTf^- , I^- , and ClO_4^- to TPFPB^- (tetrakis(pentafluorophenyl)borate)³⁰ while the donicity of the solvent S was varied in the series methylene chloride, acetonitrile, DMPU, sulfolane, DMSO,

(30)) Recent developments on large and weakly coordinating anions have been summarized by: Strauss, S. H. *Chem. Rev.* **1993**, 93, 927.

Table 1. Experimental ^{29}Si NMR Chemical Shifts and $^1J_{\text{Si-C}}$ Coupling Constants^a

	substrate ^b	solvent system ^c	$\delta^{29}\text{Si}$ (ppm)	$^1J_{\text{Si-C}}$ (Hz)	temp (K)
(#1)	Me_3SiCl	CH_2Cl_2	31.1		300
(#2)	Me_3SiCl	pyridine- <i>d</i> ₅	31.8		300
(#3)	$[\text{Me}_3\text{Si}(\text{NMI})]^+\text{Cl}^-$	none ^d	26.5		300
(#4)	$[\text{Me}_2\text{HSi}(\text{NMI})_2]^+\text{Cl}^-$	none ^d	-85.6		300
(#5)	$[\text{Me}_3\text{Si}(\text{NMI})]^+\text{Cl}^-$	CH_2Cl_2	30.1	57	300
(#6)	$[\text{Me}_2\text{HSi}(\text{NMI})_2]^+\text{Cl}^-$	CH_2Cl_2	-46.3	68	300
(#7)	Me_3SiCl	$\text{CH}_2\text{Cl}_2 + \text{HMPA-}d_{18}$ (3)	30.6		300
(#8)	Bu_3SiCl	CH_2Cl_2	33.1		300
(#9)	Bu_3SiCl	CD_3CN	32.7		300
(#10)	Bu_3SiCl	pyridine- <i>d</i> ₅	33.3		300
(#11)	Bu_3SiCl	$\text{CH}_2\text{Cl}_2 + \text{HMPA-}d_{18}$ (3)	32.2		300
(#12)	Bu_3SiCl	$\text{CH}_2\text{Cl}_2 + \text{DMSO-}d_6$ (3)	32.9		300
(#13)	Bu_3SiCl	$\text{CH}_2\text{Cl}_2 + \text{NMI}$ (2)	32.5		300
(#14)	Me_3SiOTf	CH_2Cl_2	43.7	59	300
(#15)	Me_3SiOTf	$\text{CH}_2\text{Cl}_2 + \text{sulfolane}^e$	46.6		300
(#16)	Me_3SiOTf	CD_3CN	40.7		300
(#17)	Me_3SiOTf	$\text{DMSO-}d_6$	42.8	59	300
(#18)	Me_3SiOTf	pyridine- <i>d</i> ₅	40.8	57	300
(#19)	Me_3SiOTf	DMPU	36.6		300
(#20)	Me_3SiOTf	$\text{CH}_2\text{Cl}_2 + \text{HMPA-}d_{18}$ (1)	28.2	59	300
(#21)	$\text{Me}_3\text{SiOTf}^f$	$\text{CH}_2\text{Cl}_2 + \text{HMPA-}d_{18}$ (1)	27.8		230
(#22)	Me_3SiOTf	$\text{HMPA-}d_{18}$	27.5		300
(#23)	H_3SiOTf	Et_3N	-74.1; -82.1 ^g		300
(#24)	Me_3SiI	CH_2Cl_2	9.9		300
(#25)	Me_3SiI	CD_3CN	11.9		300
(#26)	Me_3SiI	$\text{DMSO-}d_6$	42.7		300
(#27)	Me_3SiI	$\text{CH}_2\text{Cl}_2 + \text{HMPA-}d_{18}$ (3)	28.0		300
(#28)	Me_3SiI	$\text{CH}_2\text{Cl}_2 + \text{HMPA-}d_{18}$ (3)	27.6		230
(#29)	$[\text{Me}_3\text{Si}(\text{Py})]^+\text{I}^-$	none ^d	42.2		300
(#30)	$\text{Me}_3\text{SiClO}_4$	CH_2Cl_2	46.6		255
(#31)	$\text{Me}_3\text{SiClO}_4$	pyridine- <i>d</i> ₅	42.6		300
(#32)	$\text{Me}_3\text{SiClO}_4^h$	$\text{CH}_2\text{Cl}_2 + \text{HMPA-}d_{18}$ (1)	28.1		300
(#33)	$\text{Me}_3\text{SiClO}_4$	$\text{CH}_2\text{Cl}_2 + \text{HMPA-}d_{18}$ (3)	28.1		300
(#34)	$\text{Bu}_3\text{SiClO}_4$	CH_2Cl_2	44.6	59	300
(#35)	$\text{Bu}_3\text{SiClO}_4$	$\text{CH}_2\text{Cl}_2 + \text{sulfolane}^e$	46.3		300
(#36)	$\text{Bu}_3\text{SiClO}_4$	CD_3CN	45.1		300
(#37)	$\text{Bu}_3\text{SiClO}_4$	$\text{DMSO-}d_6$	41.0	59	300
(#38)	$\text{Bu}_3\text{SiClO}_4$	$\text{CH}_2\text{Cl}_2 + \text{pyridine-}d_5^e$	38.9		300
(#39)	$\text{Bu}_3\text{SiClO}_4$	$\text{CH}_2\text{Cl}_2 + \text{DMPU}$ (3)	33.8		300
(#40)	$\text{Bu}_3\text{SiClO}_4^i$	$\text{CH}_2\text{Cl}_2 + \text{HMPA-}d_{18}$ (1)	27.2	59	300
(#41)	$\text{Bu}_3\text{SiClO}_4$	$\text{CH}_2\text{Cl}_2 + \text{HMPA-}d_{18}$ (2)	27.1	60	300
(#42)	$\text{Bu}_3\text{SiClO}_4$	$\text{CH}_2\text{Cl}_2 + \text{HMPA-}d_{18}$ (3)	26.3		230
(#43)	$\text{Bu}_3\text{SiClO}_4$	$\text{CH}_2\text{Cl}_2 + \text{NMI}$ (4)	24.4	57	300
(#44)	$\text{Me}_3\text{Si}(\text{TFPB})^j$	CD_3CN	31.7 ^k		263
(#45)	$\text{Me}_3\text{Si}(\text{TFPB})^j$	$\text{CD}_2\text{Cl}_2 + \text{CD}_3\text{CN}$ (27)	28.4 ^k		213
(#46)	$\text{Me}_3\text{Si}(\text{TFPB})^j$	$\text{CD}_2\text{Cl}_2 + \text{CD}_3\text{CN}$ (1.9)	38.5 ^k		263
(#47)	$\text{Me}_3\text{Si}(\text{TFPB})^j$	$\text{CD}_2\text{Cl}_2 + \text{CD}_3\text{CN}$ (1.7)	36.7 ^k		243
(#48)	$\text{Et}_3\text{Si}(\text{TPFPB})^l$	sulfolane	58.4 ^m		300
(#49)	$\text{Et}_3\text{Si}(\text{TPFPB})^l$	CD_3CN	36.7 ^m		300
(#50)	$\text{Bu}_3\text{Si}(\text{TPFPB})^l$	CH_2Cl_2	33.4		300
(#51)	$\text{Bu}_3\text{Si}(\text{TPFPB})^l$	$\text{CH}_2\text{Cl}_2 + \text{HMPA-}d_{18}$ (1)	32.8		300
(#52)	$\text{Et}_2\text{HSi}(\text{TPFPB})^l$	CD_3CN	-19.0	71	300
(#53)	$\text{Et}_2\text{HSiClO}_4$	CH_2Cl_2	29.7	61	300
(#54)	$\text{Et}_2\text{SiHClO}_4$	CD_3CN	26.1 ⁿ		300
(#55)	$\text{Et}_2\text{HSiClO}_4^o$	$\text{CH}_2\text{Cl}_2 + \text{HMPA-}d_{18}$ (1)	15.9	61	300
(#56)	$\text{Et}_2\text{HSiClO}_4$	$\text{CH}_2\text{Cl}_2 + \text{HMPA-}d_{18}$ (2)	14.9	61	300
(#57)	$\text{Et}_2\text{HSiClO}_4$	$\text{CH}_2\text{Cl}_2 + \text{HMPA-}d_{18}$ (3)	9.9		230
(#58)	$\text{Et}_2\text{HSiClO}_4$	$\text{CH}_2\text{Cl}_2 + \text{HMPA-}d_{18}$ (4)	13.6		300
(#59)	$\text{Et}_2\text{HSiClO}_4$	$\text{CH}_2\text{Cl}_2 + \text{NMI}$ (1)	15.3	59	300
(#60)	$\text{Et}_2\text{HSiClO}_4$	$\text{CH}_2\text{Cl}_2 + \text{NMI}$ (2)	-53.4 ^p		300
(#61)	$\text{Et}_2\text{HSiClO}_4$	$\text{CH}_2\text{Cl}_2 + \text{NMI}$ (4)	-62.4	79	300
(#62)	$\text{Et}_2\text{SiHClO}_4$	$\text{CH}_2\text{Cl}_2 + \text{pyridine-}d_5$ (1)	33.4	57	300
(#63)	$\text{Et}_2\text{SiHClO}_4$	$\text{CH}_2\text{Cl}_2 + \text{pyridine-}d_5$ (4)	-24.1	74	300

^a TMS = 0 ppm as external reference. ^b Concentration = 0.4 M. ^c Values in parentheses refer to Lewis base to substrate ratio. ^d Solid-state NMR. ^e Lewis base in excess over substrate. ^f Doublet, $J(\text{Si-P}) = 9.9$ Hz. ^g Value from ref 14b. ^h Doublet, $J(\text{Si-P}) = 10.8$ Hz. ⁱ Doublet, $J(\text{Si-P}) = 14.4$ Hz. ^j Tetrakis[3,5-bis(trifluoromethyl)phenyl]borate (TFPB), $\text{B}(\text{C}_6\text{H}_3(\text{CF}_3)_2)_4^-$. ^k Value from ref 20a. ^l Tetrakis(pentafluorophenyl)borate (TPFPB), $\text{B}(\text{C}_6\text{F}_5)_4^-$. ^m Value from ref 8f. ⁿ Very broad signal $\Delta\nu_{0.5} > 40$ Hz. ^o Doublet, $J(\text{Si-P}) = 13.5$ Hz. ^p Very broad signal $\Delta\nu_{0.5} > 100$ Hz.

Table 2. Experimental ^{13}C NMR Chemical Shifts^a

	substrate ^b	solvent system ^c	$\delta^{13}\text{C}$ (ppm)
(#3)	$[\text{Me}_3\text{Si}(\text{NMI})]^+\text{Cl}^-$	none ^d	1.1
(#4)	$[\text{Me}_2\text{HSi}(\text{NMI})_2]^+\text{Cl}^-$	none ^d	1.3; 6.7
(#5)	$[\text{Me}_3\text{Si}(\text{NMI})]^+\text{Cl}^-$	CH_2Cl_2	2.2
(#6)	$[\text{Me}_2\text{HSi}(\text{NMI})_2]^+\text{Cl}^-$	CH_2Cl_2	1.8
(#14)	Me_3SiOTf	CH_2Cl_2	-0.3
(#17)	Me_3SiOTf	$\text{DMSO}-d_6$	0.7
(#18)	Me_3SiOTf	pyridine- d_5	-1.7
(#20)	Me_3SiOTf	$\text{CH}_2\text{Cl}_2 + \text{HMPA}-d_{18}$ (1)	0.2
(#34)	$\text{Bu}_3\text{SiClO}_4$	CH_2Cl_2	12.5
(#37)	$\text{Bu}_3\text{SiClO}_4$	$\text{DMSO}-d_6$	13.5
(#40)	$\text{Bu}_3\text{SiClO}_4$	$\text{CH}_2\text{Cl}_2 + \text{HMPA}-d_{18}$ (1)	13.8
(#41)	$\text{Bu}_3\text{SiClO}_4$	$\text{CH}_2\text{Cl}_2 + \text{HMPA}-d_{18}$ (2)	13.8
(#43)	$\text{Bu}_3\text{SiClO}_4$	$\text{CH}_2\text{Cl}_2 + \text{NMI}$ (4) ^e	11.7
(#52)	$\text{Et}_2\text{HSi}(\text{TPFPB})^f$	CD_3CN	5.8
(#53)	$\text{Et}_2\text{HSiClO}_4$	CH_2Cl_2	4.6
(#54)	$\text{Et}_2\text{HSiClO}_4$	CD_3CN	4.6; 5.4
(#55)	$\text{Et}_2\text{HSiClO}_4$	$\text{CH}_2\text{Cl}_2 + \text{HMPA}-d_{18}$ (1)	5.2
(#56)	$\text{Et}_2\text{HSiClO}_4$	$\text{CH}_2\text{Cl}_2 + \text{HMPA}-d_{18}$ (2)	5.8
(#59)	$\text{Et}_2\text{HSiClO}_4$	$\text{CH}_2\text{Cl}_2 + \text{NMI}$ (1)	3.9
(#60)	$\text{Et}_2\text{HSiClO}_4$	$\text{CH}_2\text{Cl}_2 + \text{NMI}$ (2) ^e	4.8, 5.2
(#61)	$\text{Et}_2\text{HSiClO}_4$	$\text{CH}_2\text{Cl}_2 + \text{NMI}$ (4)	10.4
(#62)	$\text{Et}_2\text{HSiClO}_4$	$\text{CH}_2\text{Cl}_2 + \text{pyridine}-d_5$ (1)	3.7
(#63)	$\text{Et}_2\text{HSiClO}_4$	$\text{CH}_2\text{Cl}_2 + \text{pyridine}-d_5$ (4)	8.8

^a TMS = 0 ppm as external reference. ^b Concentration of substrate 0.4 M, numbering of entries according to Table 1. ^c Values in parentheses refer to Lewis base to substrate ratio. ^d Solid-state NMR. ^e Very broad signal of NMI due to exchange. ^f Tetrakis(pentafluorophenyl)borate.

triethylamine (TEA), pyridine, HMPA, to NMI.³¹ Structures and some properties of these typical solvents are summarized in Figure 1. In Table 1, $\delta^{29}\text{Si}$ NMR chemical shifts of more than 60 $\text{R}_3\text{SiX/S}$ and $\text{R}_2\text{HSiX/S}$ systems investigated in this work are listed together with appropriate concentration and temperature information. Measured $^1J_{\text{Si-C}}$ coupling constants are given for a number of representative systems. The entries in Table 1 are ordered first according to counterions investigated and second according to the solvents used.³¹ In Table 2, ^{13}C chemical shifts of the C_1 atoms of substituents R are listed. Throughout the text, #*n* denotes the corresponding entry in Tables 1 and 2.

Useful tools in the analysis of the silyl cationic complexes **III** and **IV** are ^{29}Si and ^{13}C NMR chemical shifts and $^1J_{\text{Si-C}}$ and $^2J_{\text{Si-P}}$ coupling constants. Previous work^{10a,14a} suggests that tetracoordination at Si leads to ^{29}Si shifts in the range -80 to 110 ppm, while pentacoordinated Si complexes have shift values between -130 and -40 ppm. Formation of neutral pentacoordinated Si complexes **II** can lead to upfield shifts of 70 ppm relative to the parent silane **I**.^{10a} The ^{13}C shifts can also be useful when differentiating between tetra- and pentacoordinated Si complexes since the C_1 atoms of the alkyl substituents should have different ^{13}C shift values in tetra- and pentacoordinated Si complexes.

It is known that larger s-character of a bond orbital $\sigma_{\text{A-B}}$ leads to a larger magnitude of coupling constant $^1J_{\text{A-B}}$ than the coupling constant associated with a bond orbital with more p-character.³² Tentatively, one could assume that coordination of S forces the Si atom in R_3Si^+ to rehybridize from sp^2 to sp^3 and that, as a consequence, the SiC bond orbitals lose some s-character. However, pentacoordination in complexes $\text{R}_3\text{Si}(\text{S})_2^+$ does not require any rehybridization if one assumes that

SiS bonding in $\text{R}_3\text{Si}(\text{S})_2^+$ complexes is either electrostatic or established by S donating an electron pair to Si^+ . With these assumptions, the $^1J_{\text{Si-C}}$ coupling constants of pentacoordinated Si complexes of type **IV** with sp^2 -hybridized Si-C bonds should be larger than those of tetracoordinated Si complexes of type **III**, where the Si-C bonds are sp^3 hybridized. There is experimental evidence that suggests a dependence of $^1J_{\text{Si-C}}$ coupling constants on the degree of hybridization at both Si and C^{33a} and, accordingly, we can use this information to distinguish between type **III** and type **IV** complexes. However, one has to stress that in view of the reduced tendencies of Si to form hybrid orbitals the degree of hybridization may be used here just as a model descriptor rather than a basic fact that explains the bonding in $\text{R}_3\text{Si}(\text{S})_n^+$ complexes.³³

As mentioned in the introduction, experimentally measured ^{29}Si NMR chemical shifts are affected by the actual coordination (i.e. type of substituent R, geometry of complex, surrounding solvent shell, etc.), but also by the equilibria positions in reaction 1. For a given solvent, the equilibrium is shifted to the right of reaction 1 when the coordination ability of the anion decreases.¹⁵ Possible equilibria between structures **I-IV** can be estimated by temperature effects on the $\delta^{29}\text{Si}$ values. It is known that R_3SiX compounds are largely undissociated in CH_2Cl_2 because of the low polarity of this solvent.^{9,15} Therefore, methylene chloride solutions can serve as reference for undissociated R_3SiX (**I**). In some cases it was not possible to dissolve R_3SiX and R_2HSiX in a specific solvent S, and then R_3SiX and R_2HSiX were dissolved in binary mixtures of CH_2Cl_2 and the solvent in question.

For solutions of trialkylsilyl chlorides (#1, #2, and #7-13, Table 1), the ^{29}Si NMR chemical shifts are all between 31 and 33 ppm. No or only minor conductivity was reported for similar solutions,^{16a,34} and temperature effects on the NMR chemical shifts could not be noticed, not even for the most donating solvent HMPA. Ion pairing effects are negligible, and two-bond Si-P coupling $^2J_{\text{Si-P}}$ could not be observed in HMPA. Trialkylsilyl chlorides in solution represent neutral tetracoordinated Si species of type **I** independent of solvent conditions. A neutral pentacoordinated Si complex $\text{SiH}_3\text{Cl}(\text{OMe}_2)$ was found in the crystal state,¹⁸ while type **III** cations can be generated from R_3SiCl in the solid state if extremely potent donors such as *N*-methylimidazole (NMI) are used.²²

Contrary to trimethylsilyl chlorides, the trimethylsilyl triflate solutions #14-22 show a clear solvent dependence. Changes in the $\delta^{29}\text{Si}$ values suggest that equilibria between **I**, **II**, and **III** are formed when Me_3SiOTf is dissolved in acetonitrile or sulfolane in which substantial concentrations of the parent trimethylsilyl triflate are still present (#15 and #16). Only a slight upfield shift in the $\delta^{29}\text{Si}$ value is observed in NCCD_3 solution (40.7 ppm, #16, Table 1), compared to the reference value of 43.7 ppm obtained in methylene chloride solution (#14). The assumption of such equilibria, probably shifted strongly to **I** (**II**), is in accordance with the results of IR experiments that did not detect any stretching bands indicating the coordination of a nitrile to R_3Si^+ .^{20b}

Significant ^{29}Si shift changes are observed when dissolving Me_3SiOTf in solvents with higher donicities such as DMPU and HMPA (#19 and #20-22), for which $\delta^{29}\text{Si}$ values of 36.6 and 27.5-28.2 ppm were measured. Temperature effects could

(31) (a) Gutman, V. *Coord. Chem. Rev.* **1976**, *18*, 225. (b) Reichardt, C. *Solvents and Solvent Effects in Organic Chemistry*; VCH (Weinheim): Weinheim, Germany, 1988. (c) Hüchel, E. Z. *Phys. Chem.* **1940**, *186*, 129.

(32) (a) Muller, N.; Pritchard, D. E. *J. Chem. Phys.* **1959**, *31*, 1471. (b) Frei, K.; Bernstein, H. J. *J. Chem. Phys.* **1963**, *38*, 1216.

(33) (a) Brook, A. G.; Abdesaken, F.; Gutekunst, G.; Plavac, N. *Organometallics* **1982**, *1*, 994. See also: (b) Kovacek, D.; Maksic, Z. B.; Elbel, S.; Kudnig, J. *J. Mol. Struct. (THEOCHEM)* **1994**, *304*, 247. A clear description of the reduced tendency of Si to form hybrid orbitals can be found in: (c) Kutzelnigg, W. *Angew. Chem., Int. Ed. Engl.* **1984**, *23*, 272.

(34) Chojnowski, J.; Cypryk, M.; Michalski, J. *J. Organomet. Chem.* **1978**, *161*, C31.

not be noticed in the HMPA solutions, thus indicating that one complex type is dominant, most likely a tetracoordinated Si complex of type **III**. At low temperature (230 K) and at a 1:1 ratio of $\text{Me}_3\text{SiOTf}:\text{HMPA}$ in CD_2Cl_2 (#21), a doublet in the ^{29}Si signal due to a two-bond Si–P coupling $^2J_{\text{Si-P}}$ of 9.9 Hz was observed. This clearly shows that just one HMPA molecule is within the first coordination sphere, in line with a tetracoordinated Si complex $\text{Me}_3\text{Si}(\text{HMPA})^+$. The $\delta^{29}\text{Si}$ value of Me_3SiOTf dissolved in DMPU (36.6 ppm; #19) is close to the value obtained in N,N',N',N' -tetramethylurea (36.5 ppm).¹⁵ Furthermore, the Si–C coupling constants $^1J_{\text{Si-C}}$ are similar in the solvent-coordinated species (#17, #18, and #20) as in the original silane (#14), indicating a similar electronic environment of the Si atom.

Bassindale and co-workers showed, that for silyl compounds without any alkyl substituents on Si as in H_3SiOTf , pentacoordinated Si complexes can be formed.¹⁴ When H_3SiOTf was dissolved in TEA a strong upfield shift of 51 ppm was noticed (#23),^{14a} and the crystals formed contained a mixture of the two pentacoordinated Si complexes $\text{H}_3\text{SiOTf}(\text{TEA})$ and $\text{H}_3\text{Si}(\text{TEA})_2^+$, with ^{29}Si shifts of -74.1 and -82.1 ppm.^{14b}

For the trialkylsilyl iodides, one should expect approximately the same solvent effects as for the corresponding silyl triflate since iodides and triflates have similar Lewis basicities.³⁵ The $\delta^{29}\text{Si}$ value of 11.9 ppm for Me_3SiI in acetonitrile solution (#25, Table 1) reveals that the solution contains significant concentrations of unreacted iodide ($\delta^{29}\text{Si} = 9.9$ ppm; #24), similar to the analogous solution of Me_3SiOTf . Furthermore, the DMSO and HMPA solutions of Me_3SiI (#26–28) have ^{29}Si shifts close to those of the corresponding triflate solutions (#17, #20–22). For the pyridine complex, for which the tetracoordinated Si salt $[\text{Me}_3\text{Si}(\text{pyridine})]^+\text{I}^-$ has been proven by X-ray,²¹ a ^{29}Si shift of 42.2 ppm was obtained for the solid using CP/MAS NMR (#29). This value should be compared with a shift value of 40.8 ppm for Me_3SiOTf in pyridine solution (#18).

Therefore, the independence of the counterion (triflate or iodide) on measured $\delta^{29}\text{Si}$ values in HMPA, pyridine, and DMSO suggests that trialkylsilyl cationic species **III** are formed. The reported relative equilibrium constants for the salt formation in CH_2Cl_2 solutions are in accordance with this assumption.¹⁵ Temperature effects were not noticed for the HMPA solutions of either Me_3SiI or Me_3SiOTf (#20, #21, #27, and #28), which also suggests that additional solvent coordination to the trialkylsilyl cationic species does not occur.

For the sulfolane and acetonitrile solutions of tributylsilyl perchlorate (#35 and #36), the equilibrium is still in favor of the parent R_3SiX compound since the $\delta^{29}\text{Si}$ values (46.3 and 45.1 ppm) are close to that of $\text{Bu}_3\text{SiClO}_4$ in pure CH_2Cl_2 (44.6 ppm; #34). In addition, a ^{37}Cl NMR signal could not be detected in these systems, due to fast quadrupolar relaxation. It is well-known that ionic chloride or any Cl-containing anion with spherical symmetry leads to sharp lines (line width < 20 Hz) in the ^{37}Cl NMR spectra while broadening of the ^{37}Cl signal is typical of unsymmetrically solvated covalent chlorine compounds and suggests in the present case a covalent $\text{Bu}_3\text{Si}-\text{OClO}_3$ bonding situation or contact ion pair.³⁶

The ^{29}Si shift measurements of trimethyl and tributylsilyl perchlorate in more strongly donating solvents (#31–33 and 37–43) lead to $\delta^{29}\text{Si}$ values different from those of the original R_3SiX compounds. The pyridine and HMPA solutions of Me_3Si

SiClO_4 possess NMR chemical shifts similar to those of the corresponding triflate and iodide solutions thus suggesting tetracoordinated cationic species of type **III**. The change from Me to Bu substituents at Si causes an upfield shift in the $\delta^{29}\text{Si}$ values of approximately 2 ppm. For $\text{Bu}_3\text{SiClO}_4$ dissolved in DMSO (#37), a measured ^{37}Cl NMR line width of 3.5 Hz indicates that the counterion ClO_4^- is not within the first solvation sphere.³⁶ When dissolving the trialkylsilyl perchlorates in HMPA (#32 and #40), we observed a doublet with $^2J_{\text{Si-P}}$ coupling constants (10.8 and 14.4 Hz, respectively) similar to that found for trimethylsilyl triflate in HMPA (9.9 Hz). These coupling constants could be detected also at room temperature and indicate tetracoordinated Si complexes $\text{R}_3\text{Si}(\text{HMPA})^+$.

To test whether pentacoordinated Si complexes can be generated from tributylsilyl perchlorate, this compound was dissolved in the extremely potent donor NMI (#43). However, the resulting ^{29}Si chemical shift (24.4 ppm) is still in the range expected for a tetracoordinated Si complex of type **III**. Additional support for this type of coordination is obtained from the one-bond Si–C scalar coupling constant $^1J_{\text{Si-C}} = 57$ Hz, which is similar to the $^1J_{\text{Si-C}}$ value observed in HMPA solution (#40 and #41) or for the parent perchlorate (#34). Thus, the coupling constants for both NMI- and HMPA-coordinated Si complexes are in the range of most tetravalent trialkyl-substituted R_3SiX compounds. As we will show in the following, alkyl substituents in pentacoordinated type **IV** complexes possess ^{13}C shifts, which are about 5 ppm more downfield than those of the analogous tetracoordinated type **III** complexes. The ^{13}C shift of the C_1 atom (11.7 ppm; #43) for the complex formed when $\text{Bu}_3\text{SiClO}_4$ is dissolved in NMI solution is only slightly upfield compared to the corresponding values for the complexes formed in HMPA and DMSO solutions ($\delta^{13}\text{C} \approx 14$ ppm). Hence, it is unlikely that a pentacoordinated Si complex is formed in the NMI solution of $\text{Bu}_3\text{SiClO}_4$.

For tributylsilyl tetrakis(pentafluorophenyl)borate, $\text{Bu}_3\text{SiTPFPB}$, in pure CH_2Cl_2 , a ^{29}Si shift of 33.4 ppm was obtained (#50) which should be ascribed to formation of Bu_3SiCl .^{8h,19} This implies a reaction with the solvent, and in order to verify such a reaction, different amounts of strongly coordinating HMPA were added to the solution. Only minor ^{29}Si shift changes could be observed (#51), and since the measured ^{29}Si values are close to that of tributylsilyl chloride (#8), we support the earlier proposal of a reaction with the solvent.^{8h,19}

Previously reported ^{29}Si shifts for $\text{R}_3\text{SiTPFPB}$ dissolved in NCCH_3 and sulfolane^{8h} are different from the shift values in solutions of trialkylsilanes SiR_3X with more strongly coordinating counterions X. The reported ^{29}Si shifts thereby strongly suggest coordination of one solvent molecule to R_3Si^+ . The $\delta^{29}\text{Si}$ value of 36.7 ppm for $\text{Et}_3\text{SiTPFPB}$ in acetonitrile (#49)^{8h} is close to the value reported for the corresponding silyl species using tetrakis(3,5-bis(trifluoromethyl)phenyl)borate (TFPB) under similar conditions (28.4–38.5 ppm depending on the $\text{R}_3\text{SiX}/\text{NCCH}_3$ ratio and temperature; #44–47).^{20a} Formation of N -silylacetonitrilium ions $\text{R}_3\text{Si}(\text{NCCH}_3)^+$ would explain this observation.

Recent claims that pentacoordinated trialkylsilyl cationic species **IV** are present in acetonitrile solution^{20a} are not in accordance with the present measurements. The ^{13}C shifts in the study by Kira and co-workers are almost unchanged in the $\text{Me}_3\text{SiTFPB}/\text{NCCH}_3$ system, which is in contradiction to a downfield shift of 6.5 ppm observed for C_1 in $\text{Et}_2\text{HSi}(\text{NMI})_n^+$ when increasing n from 1 (tetracoordinated $\text{Et}_2\text{HSi}(\text{NMI})^+$, #59) to 2 (pentacoordinated $\text{Et}_2\text{HSi}(\text{NMI})_2^+$, #61) or the 5-ppm downfield shift observed for the analogous pyridine complexes (#62 and #63) (Table 2). Hence, none of the investigated

(35)) Bassindale, A. R.; Stout, T.; Taylor, P. G. *J. Chem. Soc., Perkin Trans. 2* **1986**, 227.

(36)) (a) Lindman, B.; Forsén, S. *NMR, Basic Principles and Progress*; Springer: Berlin, 1976; Vol. 12. (b) Lindman, B.; Forsén, S. *NMR and the Periodic Table*; Harris, R. K., Mann, B. E., Eds.; Academic Press: London, 1978; p 421.

Chart 1

	PISA-HF Geometry Optimizations		IGLO-HF//PISA-HF		IGLO-PISA//PISA-HF
	Me ₃ Si ⁺	Me ₂ HSi ⁺	Me ₃ Si ⁺	Me ₂ HSi ⁺	Me ₃ Si ⁺
complex III	CH ₃ CN (3)	CH ₃ CN (8)	CH ₃ CN (3)	CH ₃ CN (8)	CH ₃ CN (3)
	pyridine (4)	pyridine (9)	pyridine (4)	pyridine (9)	DMSO (5)
	DMSO (5)		DMSO (5)		sulfolane (6)
	sulfolane (6)		sulfolane (6)		
complex IV	CH ₃ CN (7)	CH ₃ CN (11)	CH ₃ CN (7)	CH ₃ CN (11)	
		pyridine (12)		pyridine (12)	

trialkylsilyl compounds shows any tendency to form pentacoordinated type **IV** complexes and this is also true in the presence of strong Lewis bases such as HMPA or NMI.

To facilitate the formation of pentacoordinated silyl cationic species, different solutions of diethylsilyl perchlorate were investigated. In CH₂Cl₂ + HMPA solution and at equal concentrations of Et₂HSiClO₄ and HMPA, a ²⁹Si shift of 15.9 ppm and a Si–P doublet with ²J_{Si–P} = 13.5 Hz was observed (#55). These data suggest a tetracoordinated Si complex Et₂HSi(HMPA)⁺ similar to the corresponding complexes of trialkylsilyl perchlorates (#32 and #40). When increasing the HMPA concentration or lowering the temperature an upfield shift of 6 ppm was induced (#55–58), which is contrary to the behavior of the trialkylsilyl compounds and suggests an equilibrium situation involving type **IV** complexes. The ²⁹Si signal broadens and the Si–P scalar coupling vanishes (#57 and #58), which is in line with a fast equilibrium between Et₂HSi(HMPA)⁺ and Et₂HSi(HMPA)₂⁺.

A more pronounced equilibrium situation was observed for the NMI solution of Et₂HSiClO₄. A ²⁹Si shift value of 15.3 ppm was obtained at equal concentrations of Et₂HSiClO₄ and NMI (#59) in accordance with a tetracoordinated type **III** complex. However, by further addition of NMI, the signal moves upfield and broadens until a limiting ²⁹Si shift with a narrow line centered at –62.4 ppm is obtained (#61). As in the titration experiments reported by Bassindale and co-workers,¹⁶ this finding is in line with a pentacoordinated type **IV** complex similar to that observed for H₃SiOTf in TEA (#23).¹⁴ In addition, the ¹J_{Si–C} coupling increases from 59 to 79 Hz (Table 1), in line with the assumed increase in s-character of sp²,sp³-hybridized Si–C bonds of a pentacoordinated Si complex.^{32,33} The ¹³C shift for the C₁ atom of the Et substituents also moves downfield by 6.5 ppm thus indicating a structural change.

Similar results as for the NMI solutions are observed for solutions of Et₂HSiClO₄ in the weaker donor pyridine. The tetracoordinated pyridine complex Et₂HSi(pyridine)⁺ gives rise to a δ²⁹Si value at 33.4 ppm and a ¹J_{Si–C} of 57 Hz (#62), while the pentacoordinated Si complex has a signal at –24.1 ppm and ¹J_{Si–C} = 74 Hz (#63). Hence, contrary to the bulky donor HMPA, pyridine is able to form pentacoordinated Si complexes with diethylsilyl perchlorates. Formation of a pentacoordinated Si complex Et₂HSi(NCCH₃)₂⁺ from Et₂HSiTPFPB can also be observed in the less strongly donating solvent NCCH₃ as is indicated by a δ²⁹Si value of –19.0 ppm and ¹J_{Si–C} coupling constant of 71 Hz (#52). Thus, it is likely that steric demand rather than donicity of the solvent affects the formation of pentacoordinated type **IV** complexes.

In summary, there seems to be an intriguing interplay between species **I–IV** in solution that depends on the nature of R, the donicity and steric bulk of S, the coordination ability of X, and other environmental effects. NMR spectroscopy can indicate what type of species exists under certain conditions; however, a detailed structural description of the S complex formed is beyond the possibility of NMR spectroscopy. For this purpose, additional information is required. We will show this in the next section by applying the NMR/ab initio/IGLO method to a number of selected cases listed in Tables 1 and 2.

3. NMR/Ab Initio/IGLO Investigations

Previous ab initio investigations have shown that the properties of R₃Si(S)_n⁺ complexes in the gas phase significantly differ from the properties of these complexes in solution.¹⁰ To get reasonable geometries, binding energies, and magnetic properties, it is necessary to consider the influence of the surrounding solvent molecules in some way within the ab initio description. In the present work, this is done by placing complexes R₃Si(S)_n⁺ inside an appropriately dimensioned cavity within a polarizable continuum that possesses the same dielectricity constant ε as the solvent in question. The SCF wave function of R₃Si(S)_n⁺ is calculated in a two-step iterative approach where in the second step the buildup of electrostatic charges caused by the electric field of R₃Si(S)_n⁺ on the surface of the cavity is considered. In this way, the electrostatic impact of the surrounding solvent with dielectricity constant ε is well represented and major changes in geometry, complex binding energies, charge distribution, and magnetic properties can be calculated. The solvent continuum method used in this work is the PISA approach of Tomasi and co-workers,³⁷ which has been extended by Reichel and Cremer³⁸ to perform IGLO³⁹ calculations with a PISA wave function.

Chart 1, summarizes the levels of theory used to investigate complexes **III** and **IV**. The notations IGLO-HF//PISA-HF and IGLO-PISA//PISA-HF indicate that IGLO calculations were performed with either PISA or Hartree–Fock (HF) wave function at PISA geometries where both IGLO and PISA start from a HF wave function (indicated by IGLO-HF and PISA-HF).

(37) (a) Miertus, S.; Scrocco, E.; Tomasi, J. *Chem. Phys.* **1981**, *55*, 117. (b) Bonaccorsi, R.; Cimraglia, R.; Tomasi, J. *J. Comp. Chem.* **1983**, *4*, 567. (c) Bonaccorsi, R.; Pala, P.; Tomasi, J. *J. Am. Chem. Soc.* **1984**, *106*, 1945. (d) Pascual-Ahuir, J. L.; Silla, E.; Tomasi, J.; Bonaccorsi, R. *J. Comput. Chem.* **1987**, *8*, 778.

(38) Reichel, F.; Cremer, D. To be published.

(39) (a) Kutzelnigg, W. *Isr. J. Chem.* **1980**, *19*, 193. (b) Schindler, M.; Kutzelnigg, W. *J. Chem. Phys.* **1982**, *76*, 1919. (c) Kutzelnigg, W.; Schindler, M.; Fleicher, U. *NMR, Basic Principles and Progress*; Springer: Berlin, 1989; Vol. 23.

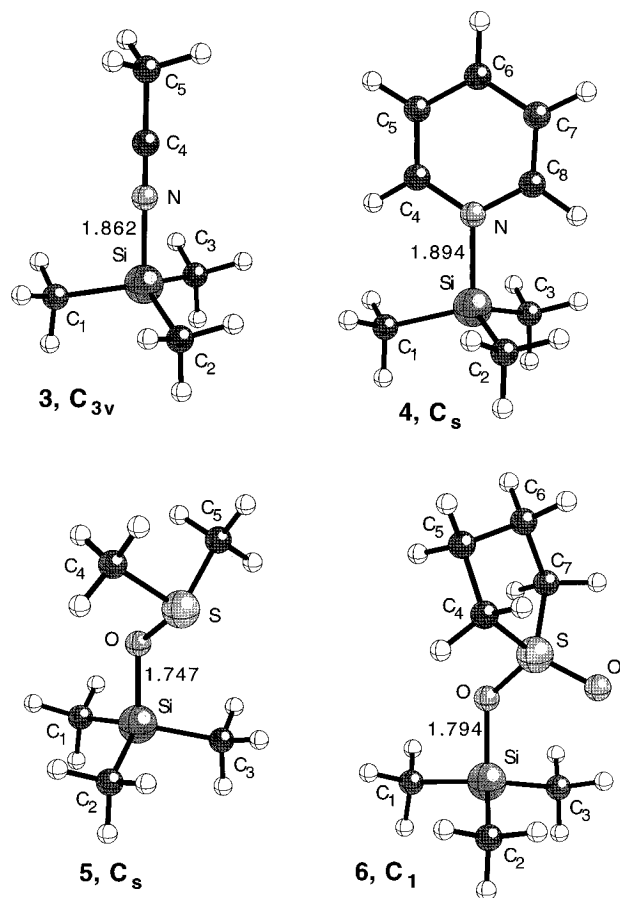
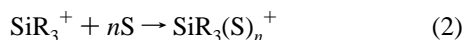


Figure 2. Optimized PISA-HF/6-31G(d) geometries of complexes $\text{Me}_3\text{Si}(\text{S})^+$ **3**–**6**. Si–S distances are given in Å.

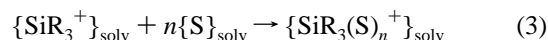
PISA-HF/6-31G(d) geometries of S complexes **3**–**6** of silylium cation Me_3Si^+ are shown in Figure 2, while complete sets of optimized geometries together with energies are given in the supporting information. A summary of the most important data of complexes **3**–**13**, namely complex binding energies, Si–S interaction distances, ^{29}Si and ^{13}C NMR IGLO chemical shifts, and charge transfer data, is given in Table 3.

All calculated Si–S distances in solution are 0.01–0.04 Å shorter than the corresponding data in the gas phase, which is easy to understand in view of the additional polarization of the complex partners caused by the surrounding solvent. This leads to a stronger charge transfer from S to Si and, hence, a shorter interaction distance accompanied by an increase of the complex binding energy, which is defined as the reaction energy of (2)



Actually, the complex binding energy derived from (2) is valid for the gas phase, which differs from that in the solution phase (reaction 3) since the reference point for the latter is not a naked but a solvated silylium cation where the solvation shell leads

to considerable stabilization and, therefore, to a less strong



change in energy upon complex formation. As a consequence, complex binding energies in solution are 10–20 kcal/mol smaller than those in the gas phase. Also, complexation with a second S molecule leads to almost no additional stabilization in solution (Table 3) and, therefore, complex binding energies of $\text{SiR}_3(\text{S})_2^+$ in gas and solution phases differ even more (20–30 kcal/mol) than the corresponding values of complexes $\text{SiR}_3(\text{S})^+$.

The calculated distances of all complexes investigated are just slightly longer than the corresponding covalent bond distances in compounds SiR_3AH_m ($\text{A} = \text{O}, \text{N}; m = 1, 2$) where A is the directly coordinating atom in $\text{SiR}_3(\text{S})_n^+$ complexes. Investigations of the electron density distribution⁴⁰ of $\text{SiR}_3(\text{S})_n^+$ indicate at least weak covalent bonding in cationic complexes **3**–**13**. This is only possible by a considerable transfer of negative charge (Table 3) from S to SiR_3^+ accompanied by the formation of a covalent bond between Si and A of S. In this way, the silylium cation character is lost and silylnitrilium, -iminium, or -oxonium ions are formed. This is discussed in more detail in the following.

$\text{Me}_3\text{Si}(\text{NCCH}_3)_n^+$ Complexes **3 and **7**.** The Si–N bond distance of complex **3** in acetonitrile solution is 1.86 Å (Figure 2), which is only slightly longer than a typical covalent Si–N bond distance of 1.71–1.74 Å.⁴¹ The strength of the Si–N bond is reflected by a complex binding energy of 39.5 kcal/mol. The IGLO-HF/PISA-HF $\delta^{29}\text{Si}$ value of **3** is 42.8 ppm, which is significantly larger than measured shift values of 28.4 (#45, Table 1) to 38.5 ppm (#46).^{8b,20} However, IGLO-PISA/PISA-HF calculations lead to a shift value of 35.7 ppm in accordance with the experimental shift values of Me_3SiTFPB and $\text{Et}_3\text{SiTPFPB}$ in pure acetonitrile (31.7 ppm, #44; 36.7 ppm, #49, Table 1). An exact adjustment of calculated and experimental $\delta^{29}\text{Si}$ value (#44, Table 1) within an NMR/ab initio/IGLO approach leads to a negligible change in the Si–N distance. This means that a reasonable account of the geometry of **3** in acetonitrile solution by the PISA method and the direct consideration of solvent effects on chemical shifts by IGLO-PISA is sufficient to describe the magnetic properties of the complex and, by this, also its geometry and binding energy correctly. The variation of $\delta^{29}\text{Si}$ with the solvent dielectricity ϵ is moderate but non-negligible. For $\epsilon = 10$ (CH_2Cl_2), a value of 37.8 ppm is calculated which is in line with variations in the experimental shift value depending on the experimental conditions (#44–47). In any case, acetonitrile forms a relatively strong tetracoordinated Si complex of type **III** that is closer to a covalently bonded R_3SiX ($\text{X} = \text{NR}'_2$) compound than to a cation R_3Si^+ .

The type **IV** complex **7** is most stable in the C_{3v} symmetrical form **7a**, in which one CH_3CN molecule is closely attached to Si while the second CH_3CN molecule sits at a Si–N distance of 3.3 Å. In other words, **7a** can be regarded as **3** which is loosely coordinated by a second CH_3CN molecule. The IGLO-HF/PISA-HF ^{29}Si shift value of **7a** (40.6 ppm) is closer to experimental values than that of **3** (42.8 ppm) which simply reflects the fact that solvent effects on the NMR chemical shifts can be covered by a IGLO-PISA calculation with the appropriate dielectricity constant or by IGLO-HF calculations for super-complexes that incorporate successively the surrounding solvent shell. Clearly, one has to include the whole solvation shell in the IGLO-HF calculation to get an acceptable correspondence

(40) (a) Cremer, D.; Kraka, E. *Croat. Chem. Acta* **1984**, 57, 1259. (b) Cremer, D.; Kraka, E. *Angew. Chem., Int. Ed. Engl.* **1984**, 23, 62. (c) Kraka, E.; Cremer, D. In *Theoretical Models of the Chemical Bond, Part 2: The Concept of the Chemical Bond*, Maksic, Z. B., Ed.; Springer: New York, 1990; p 453. (d) Cremer, D. In *Modelling of structure and properties of molecules*; Maksic, Z. B., Ed.; Ellis Horwood: Chichester, England, 1988; p 125. (e) Cremer, D.; Kraka, E. In *Molecular Structure and Energetics, Structure and Reactivity*; Liebman, J. F., Greenberg, A., Eds.; VCH Publishers: Deerfield Beach, FL, 1988; Vol. 7, p 65. (f) Cremer, D. *Tetrahedron* **1988**, 44, 7427.

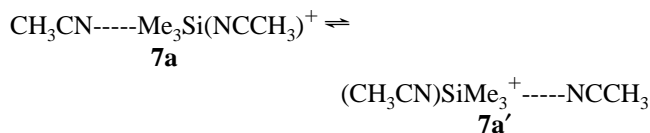
(41) (a) Shieldrick, W. S. In *The Chemistry of Organosilicon Compounds*; Patai, S., Rappoport, Z., Eds.; Wiley Interscience: New York, 1989; p 227.

Table 3. Calculated Complex Binding Energies, Bond Lengths, ^{29}Si and ^{13}C NMR Chemical Shifts, and Charge Transfer Values^a

	molecule	sym	<i>I</i>	ϵ	complexation energy	distance Si—S	$\delta^{29}\text{Si}$	$\delta^{13}\text{C}$	charge transfer	SiS bonding
(1)	SiMe_3^+	C_{3h}	0				355.9	9.0		
(2)	SiHMe_2^+	C_{2v}	0				334.1	9.8		
(3)	$\text{SiMe}_3(\text{NCCH}_3)^+$	C_{3v}	0	37.5	39.5	1.862	42.8, 35.7	-1.0	0.320	covalent
(4)	$\text{SiMe}_3(\text{pyridine})^+$	C_s	0	12.3	52.6	1.894	45.1	-1.1 ^b	0.336	covalent
(5)	$\text{SiMe}_3(\text{DMSO})^+$	C_s	0	46.7	58.9	1.747	47.0, 45.0	-1.0 ^b	0.352	covalent
(6)	$\text{SiMe}_3(\text{sulfolane})^+$	C_1	0	43.3	41.4	1.794	58.9, 58.3	-0.4 ^b	0.303	covalent
(7a)	$\text{SiMe}_3(\text{NCCH}_3)_2^+$	C_{3v}	0	37.5	39.6	1.866 3.310	40.6	-1.0	0.314 0.029	covalent no bond
(7b)	$\text{SiMe}_3(\text{NCCH}_3)_2^+$	C_{3h}	1	37.5	34.1	2.172	3.4	3.6	0.235	weak covalent
(8)	$\text{SiHMe}_2(\text{NCCH}_3)^+$	C_s	0	37.5	43.7	1.849	18.4	-3.2	0.347	covalent
(9)	$\text{SiHMe}_2(\text{pyridine})^+$	C_s	0	12.3	58.8	1.870	33.6	-2.0	0.364	covalent
(10)	$\text{SiHMe}_2(\text{NMI})^+{}^c$	C_1	0		83.5	1.856	14.0	-2.7 ^b	0.375	covalent
(11)	$\text{SiHMe}_2(\text{NCCH}_3)_2^+$	C_2	0	37.5	43.8	2.103	-47.5	0.6	0.299	weak covalent
(12)	$\text{SiHMe}_2(\text{pyridine})_2^+$	C_2	0	12.3	61.2	2.106	-38.1	3.1	0.359	weak covalent
(13)	$\text{SiHMe}_2(\text{NMI})_2^+{}^c$	C_2	0		101.0	2.079	-63.9	4.9	0.376	weak covalent

^a *I*: Number of imaginary frequencies. ϵ : dielectricity constant. Complexation energies [kcal/mol] calculated at the PISA-HF/6-31G(d) level for the reaction $\text{SiR}_3^+ + n\text{S} \rightarrow \text{SiR}_3(\text{S})_n^+$ ($n = 1$ or 2). Distances between Si and coordinating atom of solvent molecule S in Å. NMR shift values [in ppm relative to TMS] calculated at the IGLO-HF/[7s6p2d/5s4p1d/3s1p]/PISA-HF/6-31G(d) level of theory. Values in italics calculated at the IGLO-PISA/[7s6p2d/5s4p1d/3s1p]/PISA-HF/6-31G(d) level. Charge transfer values [in electron] give the transfer of negative charge from S to Si. The covalent character of SiS bonds was determined according to criteria given by Cremer and Kraka.⁴⁰ ^b Averaged ^{13}C shifts for the methyl substituents. ^c Calculated at the HF/6-31G(d) and IGLO-HF/[7s6p2d/5s4p1d/3s1p]/HF/6-31G(d) level.

with experimental ^{29}Si shifts.



The pentacoordinated form **7b** corresponds to the transition state of a degenerate exchange of the two CH_3CN molecules in **7a** to lead to **7a'**. Since the barrier for this reaction is just 5.5 kcal/mol (Table 3), there will be rapid equilibrium at temperatures down to 200 K, which have been realized in experiments.¹⁹ This could provide a model for the actual situation of **3** being surrounded by a solvent shell: The shape of the solvent shell rapidly changes because of contraction on one side and complementary expansion on the opposite side caused by replacement of the tightly bound solvent molecule in **3** by a solvent molecule out of the solvent shell. In this way, properties of the solvent molecules are averaged over different positions in the solvent shell and R_3Si^+ ion.

The investigation of **3** and **7** clearly shows that cation **1** or any trialkylsilylium cation R_3Si^+ can form just tetracoordinated type **III** complexes while type **IV** complexes are kinetically not stable and only occur in connection with degenerate rearrangements within the solvent shell. This is in line with experimental observations that give no indication of type **IV** complexes of R_3Si^+ ions in acetonitrile. Test calculations show that the same conclusions can be drawn for cation **1** in more nucleophilic solutions. Type **IV** complexes seem to be important just in connection with degenerate rearrangement processes between tetracoordinated type **III** complexes. Indeed, such a degenerate rearrangement was observed for the $\text{Me}_3\text{Si}(\text{OEt}_2)^+$ complex by Kira and co-workers.¹⁹

$\text{Me}_3\text{Si}(\text{S})^+$ Complexes 4, 5, and 6. The Si—S distances of **4**, **5**, and **6** vary between 1.75 and 1.89 Å (Figure 2) and, accordingly, are merely 0.10–0.20 Å longer than normal Si—N and Si—O bonds.⁴¹ It is interesting to note that the Si—N bond lengths reported for the crystal geometries of $\text{Me}_3\text{Si}(\text{pyridine})^+$ ²¹ and $i\text{-Pr}_3\text{Si}(\text{NCCH}_3)^+$ ^{13d} are shorter by 0.03–0.04 Å than those calculated at the PISA-HF level. Similar deviations were reported by Gordon and co-workers when comparing X-ray

crystal data on silatranes with geometries calculated using a solvent continuum model.⁴²

Si—S distances and binding energies of **4**, **5**, and **6** reveal that the complex properties are not necessarily parallel to the donicity of the solvent molecule S (Figure 1). For example, the donicity of pyridine is larger than that of DMSO; however, the complex binding energy of **5** (59 kcal/mol, Table 3) is about 6 kcal/mol larger than that of **4** (52.6 kcal/mol, Table 3). Inspection of Figure 2 reveals that **4** suffers from steric interactions between the methyl groups of R_3Si^+ and the CH bonds in the α -position of the N atom. Steric interactions are absent in both **3** and **5** (Figure 2) while they are present in **4** and **6**. Hence, binding energies and Si—S distances (Table 3) reflect not just the donicity or nucleophilic character of S but also steric factors relevant for the approach of S to R_3Si^+ .

The IGLO-HF//PISA-HF $\delta^{29}\text{Si}$ value of **4** is 45.1 ppm, which decreases however to 39.8 ppm if the reported X-ray geometry of $\text{Me}_3\text{Si}(\text{pyridine})^+$ ²¹ is used. This is in reasonable agreement with the observed shift values for Me_3Si^+ in pyridine solutions (40.8–42.6 ppm; #18 and 31, Table 1) or the experimental CP/MAS value of 42.2 ppm for solid **4** (#29). In the latter case, PISA calculations are not adequate since (a) the choice of the dielectricity constant is difficult and (b) the environment of **4** is ordered and should be described by crystal HF calculations. IGLO-PISA calculations only lead to a marginal decrease of the $\delta^{29}\text{Si}$ value while a reduction of the Si—N bond length to 1.884 Å helps to reproduce experimental $\delta^{29}\text{Si}$ values of #18 and #31.

For complex $\text{Me}_3\text{Si}(\text{DMSO})^+$ (**5**) a ^{29}Si shift of 47.0 ppm is calculated at the IGLO-HF//PISA-HF level of theory, which decreases to 45.0 ppm if solvent effects on the ^{29}Si shift are directly considered at the IGLO-PISA//PISA-HF level of theory. This is within 2 ppm of the experimental values (42.7–42.8 ppm; #17 and 26). A small reduction of the SiO distance leads to an exact agreement between experimental and calculated shift values.

For $\text{Me}_3\text{Si}(\text{sulfolane})^+$ (**6**), $\delta^{29}\text{Si}$ values of 58.9 and 58.3 ppm are calculated at the IGLO-HF and IGLO-PISA levels of theory where the small solvent effect of 0.6 ppm seems to be a result of the bulkiness of sulfolane and a relatively large distance between soluted complex and the solvation shell formed by

(42) Schmidt, M. W.; Windus, T. L.; Gordon, M. S. *J. Am. Chem. Soc.* **1995**, *117*, 7480.

sulfolane molecules. Both IGLO values are in good agreement with the experimental $\delta^{29}\text{Si}$ value of 58.4 ppm measured for $\text{Et}_3\text{SiTPFPB}$ in sulfolane (#48). The data in Table 1 suggest that replacement of Me groups by Et groups in $\text{R}_3\text{Si}(\text{sulfolane})^+$ leads to a decrease by 2–3 ppm to about 56 ppm. Again, this value can be reproduced by a relatively small reduction of the SiO distance.

For complexes **4**, **5**, and **6**, NMR/ab initio/IGLO calculations confirm the formation of tetracoordinated type **III** complexes between R_3Si^+ and pyridine, DMSO and sulfolane (see Figure 2) for counterions with less coordinating ability than OTf^- and I^- such as ClO_4^- and TPFPB^- . For sulfolane and CH_3CN , complexes of type **III** were only formed when the TPFPB^- anion was used as counterion. Complex binding energies, SiS distances, charge transfer data, and electron density distributions between Si and S suggest significant covalent SiS bonding and a loss of silylium cation character.

$\text{Me}_2\text{HSi}(\text{S})^+$ Complexes **8, **9**, and **10**.** Experiments indicate that tetracoordinated type **III** complexes are formed when $\text{Et}_2\text{HSiClO}_4$ and $\text{Et}_2\text{HSiTPFPB}$ are dissolved in nucleophilic media. In the case of strong nucleophilic or sterically less demanding solvents, a second S molecule can coordinate and an equilibrium between type **III** and type **IV** complexes is established (#55–58, Table 1). With an excess of acetonitrile (counterion TPFPB , #52), pyridine, or NMI (counterion ClO_4^- , #59–63, Table 3), pentacoordinated type **IV** complexes dominate.

The binding energies of complexes **8** and **9** (43.3 and 58.9 kcal/mol, Table 3) are 4–6 kcal/mol stronger and the distances Si–S (1.849 and 1.870 Å) are 0.01–0.02 Å shorter than in the corresponding complexes of cation **1**. Also, the charge transfer from S to Si is larger indicating that R_2HSi^+ is more electrophilic than R_3Si^+ in solutions of nucleophilic solvents. The reason for the increased electrophilicity has to do with the electron-donating power of a methyl group. In **1**, three methyl groups donate negative charge to the $3p\pi$ orbital of the Si atom by hyperconjugation while in **2** just two methyl groups are available for hyperconjugation. As a consequence, the $3p\pi$ orbital of Si is less populated in **2** than in **1** thus being more prone for interactions with a nucleophilic partner S. This is also reflected by the calculated $\delta^{29}\text{Si}$ values of **8** and **9**, which are shifted 10–25 ppm upfield relative to **3** and **4**. However, it has to be noted that the actual $\delta^{29}\text{Si}$ value is a result of σ - and π -effects, i.e. inductive and hyperconjugative effects, as well as diamagnetic and paramagnetic shielding effects. For example, each methyl group influences Si not just by a hyperconjugative effect involving the $3p\pi$ orbital but also by inductive (electron withdrawing) effects involving $3p\sigma$ orbitals. The latter predominate in **1** and **2**, and as a consequence, **1** possesses a more positive $\delta^{29}\text{Si}$ value than **2**.

For complex **8**, $\text{Me}_2\text{HSi}(\text{NCCH}_3)^+$, the calculated $\delta^{29}\text{Si}$ value (18.4 ppm, Table 3) is 8 ppm larger than the measured value for $\text{Et}_2\text{HSiClO}_4$ in acetonitrile (26.1 ppm; #54). Even if one considers the change in the shift value caused by replacing methyl by ethyl groups, the difference between observed and calculated $\delta^{29}\text{Si}$ value suggests that an equilibrium between a type **III** complex and a substantial amount of $\text{Et}_2\text{HSiClO}_4$ exists as indicated by the Si line broadening, where the latter species has a shift value of 29.7 ppm (#53, Table 1).

In the case of complex **9**, $\text{Me}_2\text{HSi}(\text{pyridine})^+$, the IGLO $\delta^{29}\text{Si}$ value of 33.6 ppm is close to the corresponding value of $\text{Et}_2\text{HSiClO}_4$ dissolved in pyridine (33.4 ppm; #62). A similarly good agreement between IGLO (14.0 ppm, Table 3) and measured $\delta^{29}\text{Si}$ shift (15.3 ppm, #59, Table 1) is obtained for complex **10**, $\text{Et}_2\text{HSi}(\text{NMI})^+$. Hence, in both cases, tetracoordinated type **III** complexes exist under the conditions of the

NMR experiments described in the previous section. Complexes **9** and **10** present reasonable models for the $\text{Et}_2\text{HSi}(\text{S})^+$ complexes investigated in solution.

$\text{Me}_2\text{HSi}(\text{S})_2^+$ Complexes **11, **12**, and **13**.** Contrary to cation **1**, cation **2** forms pentacoordinated type **IV** complexes of significantly increased stability with strong nucleophilic solvents which are not sterically hindered. In the case of complex **11**, acetonitrile does not possess a sufficiently high donicity to form strong bonds between Si and the two CH_3CN molecules. Pentacoordinated complexes could be observed but only when TPFPB is used as counterion (#52) and provided that the substituents R are not sterically demanding. However, contrary to **7** the acetonitrile molecules occupy equivalent positions in the complex thus leading to overall C_2 symmetry of the complex ion. The SiN distances are both 2.1 Å and, by this, more than 0.2 Å longer than the close contact distances between S and Si in **3** and **7a**. However, the SiN distance in **11** is still 0.5 Å shorter than the average SiN distance in **7a** (2.6 Å) and even 0.07 Å shorter than the SiN distances in TS **7b**. This is also reflected by the calculated complex binding energy (43.8 kcal/mol), which is 4 kcal/mol larger than in **7a** although it does not differ from that of **8**.

For complexes **12** and **13**, the increase in stability due to complexation by two rather than one solvent molecule is more pronounced as is reflected by binding energies of 61 and 101 kcal/mol, respectively. Actually, the SiN distances are slightly larger for **12** than for **11**, which again reflects the fact that the larger donicity of pyridine is partially offset by steric repulsion that hinders tight SiN binding in the complex. In general, a SiS distance, which is 0.2 to 0.25 Å longer than the SiS distance of a type **III** complex, has to be expected upon formation of a type **IV** complex of R_2HSi^+ .

The IGLO $\delta^{29}\text{Si}$ values for **11** and **12** (–47.5 and –38.1 ppm) are upfield by 28 and 14 ppm with regard to the $\delta^{29}\text{Si}$ shift values measured for Et_2HSiX in acetonitrile and pyridine solution (–19 ppm, #52; –24.1 ppm, #63, Table 1). However, a change in the alkyl groups of R_2HSiX has a large effect on the $\delta^{29}\text{Si}$ values of pentacoordinated complexes as is suggested by a downfield shift of 19 ppm obtained for $\text{Me}_2\text{HSi}(\text{NMI})_2^+$ ($\delta^{29}\text{Si}$ = –81 ppm)¹⁶ and $\text{Et}_2\text{HSi}(\text{NMI})_2^+$ (–62.4 ppm, #61). If this shift difference is used to estimate $\delta^{29}\text{Si}$ values for type **IV** complexes of Et_2HSiX in acetonitrile and pyridine, then shifts of –29 and –19 ppm will be obtained, which differ by 10 and 5 ppm from experimental values. At the moment, it cannot be judged whether the remaining differences are due to deficiencies of the theory (because of computational limitations IGLO-PISA calculations could not be performed) or indicate in the case of acetonitrile an equilibrium between $\text{Et}_2\text{HSi}(\text{NCCH}_3)^+$ and $\text{Et}_2\text{HSi}(\text{NCCH}_3)_2^+$ ions. The observed $^1J_{\text{Si-C}}$ give some support for the latter proposal as well as the C_1 shift (#52).

Similar reservations have to be made with regard to the calculated ^{29}Si shift of **13** (–64 ppm), which could only be obtained at the IGLO-HF/HF level of theory, i.e. without any consideration of solvent effects. For **13** in the solid state, a shift of –86 ppm is measured (#4, Table 1), while Bassindale and co-workers report a shift of –81 ppm in solution.^{16b} Considering the fact that one calculates an upfield shift of 14 ppm in the case of **11** when going from the gas phase to an acetonitrile solution and considering that the calculated SiN distances are 0.05–0.08 Å longer in the gas phase than those measured in the crystal,²² an IGLO-HF/PISA-HF value of –78 ppm in close agreement with experimental values can be predicted. In view of this value, the $\delta^{29}\text{Si}$ value of –46 ppm and the $^1J_{\text{Si-C}}$ coupling constant of 68 Hz obtained when dissolving $\text{Me}_2\text{HSi}(\text{NMI})_2^+$

crystals in CH_2Cl_2 suggest an equilibrium between type **III** and type **IV** complexes or even the formation of a type **II** complex.

At this time, it is appropriate to discuss the downfield shifts of 5–7 ppm in $\delta^{13}\text{C}$ values (Table 2) for the C_1 atoms of the ethyl groups when replacing $\text{Et}_2\text{HSi}(\text{S})^+$ by $\text{Et}_2\text{HSi}(\text{S})_2^+$. For S = pyridine (#62 and 63), theory predicts a difference between the corresponding $\delta^{13}\text{C}$ values of **9** and **12** of 5.1 ppm (Table 3) in agreement with the experimental value of 5 ppm. Similar differences in ^{13}C shifts are calculated between **8** and **11** (3.8 ppm, Table 3) as well as between **10** and **13** (7.6 ppm, Table 3; 6.5 ppm, #59 and 61, Table 2). Although these differences are not very large, they can be used to distinguish between type **III** and type **IV** complexes of R_2HSi^+ cations.

4. Conclusions

The combination of NMR measurements on a large number of R_3SiX solvent and R_2HSiX solvent systems and NMR/ab initio/IGLO investigations has led to a number of interesting results which considerably improve the knowledge about the properties of silylium cations in solution. These results can be summarized as follows.

(1) Theory reveals that complex formation of silylium cations in solution can be understood as the result of three factors, namely, steric effects concerning both R and S , internal stabilization of the silyl cation via hyperconjugation, and external stabilization via S coordination. With an increasing number of alkyl groups, the silylium cation is internally stabilized by hyperconjugation leading to the transfer of negative charge into the empty $3p\pi$ orbital of Si . Therefore, trialkylsilylium cations R_3Si^+ such as Me_3Si^+ stabilize themselves by forming tetra-coordinated type **III** complexes with sufficiently strong nucleophilic solvents (donicity ≥ 10), however, they do not form pentacoordinated type **IV** complexes. Pentacoordination of Si occurs only in the transition state of degenerate S exchange reactions, in which a tightly bonded S molecule changes place with one of the S molecules of the solvent shell.

For R_2HSi^+ and accordingly also for RH_2Si^+ and H_3Si^+ , the formation of pentacoordinated type **IV** complexes is possible since internal stabilization by two or one alkyl group is much weaker and increases the electrophilicity of the Si atom. With the NMR/ab initio/IGLO method we have proven the existence of type **IV** complexes in solutions of acetonitrile, pyridine, and NMI.

(2) Although the donicity of a solvent molecule is an important factor that determines complex formation and complex stability, there are several other factors that strongly influence the properties of an S complex of silylium cations in solution. In particular, the steric bulk of a solvent molecule S can significantly reduce its complex-forming ability. This was observed in the case of pyridine (steric repulsion with the α -H atoms) and sulfolane, but is also important in the case of DMPU or NMI. Steric effects are especially important for the formation of pentacoordinated complexes as exemplified by the formation of **IV** with acetonitrile but not with HMPA.

The dielectricity constant of the solvent influences the formation of a solvent shell and electrostatic interactions between solvent shell and soluted complex. This is reflected by the PISA calculations, which indicate relatively large changes in geometry and $\delta^{29}\text{Si}$ chemical shifts upon solvation (solvent shell formation) in solvents with relatively large ϵ values (acetonitrile:3; DMSO:5; sulfolane:6).

The impact of the counterion is another important factor, which influences complex formation. In this work, it has been studied by systematic NMR measurements on five different counterions. Decreasing coordination ability in the series Cl^- ,

$\text{I}^- \approx \text{TfO}^-$, ClO_4^- , TPFPB^- has been observed, i.e. complex formation is most likely if the coordinating ability is small as in the case of TPFPB^- anions.

(3) In a number of cases (#6, #15, #16, #25, #35, #36, and #55–58), measured NMR chemical shifts as well as chemical shift calculations clearly indicate the existence of an equilibrium either between **I** (and/or **II**) and **III** or between **III** and **IV**. Scalar coupling constants gave additional information on the coordination number.

(4) Using the NMR/ab initio/IGLO method, we have obtained complex binding energies, charge distributions and geometries of complexes **3–9** in solution while for complexes **10–13** the available experimental data or the level of theory applied in this work is not sufficient to provide an exact description by the NMR/ab initio/IGLO method. We have demonstrated that accurate data can only be obtained if solvent effects are considered for both the geometry optimization and the chemical shift calculation. For this purpose, the PISA method has been used in this work, which proved to be quite satisfactory.

(5) Compared to the gas phase, calculated SiS distances for complexes $\text{R}_3\text{Si}(\text{S})_n^+$ and $\text{R}_2\text{HSi}(\text{S})_n^+$ ($n = 1$ or 2) are 0.01–0.04 Å shorter in solution, which is due to an increased polarization of both S and silylium cation within the solvent shell and, thereby, a stronger transfer of negative charge from the complex partner S to the silylium cation. Calculated SiS distances are just 5–10% longer than the corresponding covalent bond distances in neutral reference compounds.

Complex binding energies are considerably smaller in solution than in the gas phase, which simply has to do with the fact that a silylium cation surrounded by a solvent shell (reference point for the complex binding energies in solution) is much more stable than a naked silylium cation in the gas phase. Calculated binding energies in solution range from 40 to 60 kcal/mol where an increase in binding energies is parallel to an increase in solvent donicity provided steric factors do not hinder a closer contact as for example in the case of the pyridine complexes **4**, **9**, and **12**.

(6) According to the results of the electron density analysis, there are covalent SiS bonds in all cases considered. This means that neither formally nor practically can complexes **3–13** or in general $\text{R}_3\text{Si}(\text{S})_n^+$ and $\text{R}_2\text{HSi}(\text{S})_n^+$ ($n = 1$ or 2) be considered as free or nearly free silylium cations.

5. Experimental Section

All NMR spectra were recorded using Bruker AC-P 250, AMX2-500, and MSL-100 NMR spectrometers. ^{29}Si -NMR spectra were acquired by inverse gated decoupling or a DEPT pulse sequence. All chemical shifts are reported relative to external TMS. The estimated error in chemical shifts is ± 0.2 ppm. Solute concentration was kept constant at 0.4 M in all experiments. Experimental manipulations were carried out using standard inert atmosphere techniques and solutions were prepared under argon atmosphere. NMR tubes were closed with rubber septa or sealed off. The solvents were of p.a. quality and dried very carefully by standard procedures as below. Linde type 4 Å molecular sieves (Union Carbide) were used as drying agents.

Solvents. CH_2Cl_2 (Kebo Lab) was shaken with portions of concentrated H_2SO_4 until the acid layer was colorless, then washed with water, aqueous 5% Na_2CO_3 , then finally water. Thereafter the solvent was predried with CaCl_2 , distilled from CaH_2 , and stored over molecular sieves. Sulfolane (Merck) was distilled from NaOH . The distillate was in contact with CaH_2 for 48 h and distilled through a column into a bottle containing molecular sieves. The distillation procedure was repeated twice. CD_3CN ultra pure (Dr. Glaser AG Basel) was stirred over CaH_2 at gentle reflux overnight, then distilled and stored over molecular sieves. Pyridine- d_5 ultra pure (Dr. Glaser AG Basel) was dried by refluxing with BaO , followed by distillation and storing over molecular sieves. HMPA- d_{18} ultra pure (Stohler Isotope Chemi-

cals) was refluxed over BaO at 1 mmHg for several hours, then distilled from sodium at reduced pressure into a bottle containing molecular sieves. DMSO-*d*₆ ultra pure (Dr. Glaser AG Basel) was dried over CaH₂, then distilled at low pressure to molecular sieves. DMPU (Aldrich) was allowed to stand over molecular sieves for 1 day, then distilled from CaH₂ to molecular sieves. NMI (Acros Chimica) was refluxed and distilled from CaH₂ to molecular sieves under argon.

Substrates. Me₃SiCl (Aldrich) and Bu₃SiCl (Aldrich) were distilled from CaH₂. Me₃SiOTf (Aldrich), Me₃SiI (Aldrich), and Me₃SiH (ABCR GmbH & Co.) were used directly without any further purifications. Bu₃SiH (Aldrich) and Et₂SiH₂ (PCR Incorporated) were distilled from LiAlH₄ under argon prior to use. Trityl perchlorate (Ph₃C⁺ClO₄⁻) and triphenylcarbenium tetrakis(pentafluorophenyl)borate (Ph₃C⁺TPFPB⁻) were prepared according to earlier reported procedures.^{43,44} For the solid pyridine complex, 285 μL of Me₃SiI was added to 10 mL of dry pyridine in a 25-mL flask equipped with an argon inlet tube. After the solution was stirred for 1 hour, a white solid was precipitated. The excess pyridine was removed by a double needle technique and the solid was placed under high vacuum for 1 hour. The white crystals were packed in a zircon rotor in a drybox. [Me₃Si(NMI)]⁺Cl⁻ and [Me₂HSi(NMI)₂]⁺Cl⁻ were prepared as in previous reported methods.²²

Hydride-Transfer Experiments. #30–43 and #53–63 were prepared by successive addition of 1 equiv of silane (exception Me₃SiH which is weighed carefully after condensation) to a solution of 1 equiv of Ph₃C⁺ClO₄⁻ in the desired solvent, followed by the addition of the different Lewis bases. The stirring of the solutions was continued for 30 min under argon. The NMR samples were prepared by a double needle technique. Measurements were made immediately upon preparation.

#50–52 were prepared in a similar way but using Ph₃C⁺TPFPB⁻.

Computational Methods. Geometries of **1–13** were first optimized at the HF level using the 6-31G(d) basis set of Pople and co-workers.⁴⁵ Frequencies were determined at the same level of theory to check the nature of the stationary points calculated. Thereafter, geometry optimization was repeated with the PISA continuum model developed by Tomasi and co-workers³⁷ where for each solvent considered the appropriate dielectricity constant was used (see Figure 1). Test calculations for smaller complexes in solution revealed that the most sensitive parameter is the SiS distance while all other geometrical parameters change independent of the SiS distance.^{28a,46} Therefore, we developed an geometry optimization procedure in which for each SiS distance all other geometrical parameters are optimized at the HF/6-31G(d) level of theory. For *n* SiS distances calculated at the PISA/6-31G(d) level of theory, a polynomial of degree *n* – 1 was fitted to the corresponding energy points and the minimum energy was determined by standard procedures. The final HF/6-31G(d) geometry obtained for this SiS distance is identical with the true PISA/6-31G(d)

geometry within 0.002 Å and 0.2° for all test cases considered. Accordingly, this procedure was used throughout this work to obtain PISA geometries for R₃Si(S)_{*n*}⁺ and R₂HSi(S)_{*n*}⁺ (*n* = 1 or 2) cations. Geometries obtained in this way are denoted as PISA-HF/6-31G(d) to distinguish them from PISA calculations that also include correlation corrections.

All ¹³C and ²⁹Si NMR chemical shifts were calculated with the IGLO method (Individual Gauge for Localized Orbitals) of Kutzelnigg and Schindler.³⁹ In all IGLO calculations, we used a [7s6p2d/5s4p1d/3s1p] TZ+P basis set, which Kutzelnigg and Schindler designed for ¹³C and ²⁹Si NMR shift calculations.^{39c} Two different sets of IGLO calculations were carried out, namely one based on a HF wave function to obtain gas-phase values (IGLO-HF) and one based on the PISA wave function to obtain chemical shifts for solution situations (IGLO-PISA). In all cases, TMS was used as an appropriate reference for both ¹³C and ²⁹Si shift values.

The analysis of the electron density distribution was carried out along the lines described by Cremer and Kraka.⁴⁰ These authors gave criteria for describing atom, atom interactions as nonbonded, electrostatic, ionic, or covalent. The following criteria must be fulfilled for a covalent bond between atoms A and B:

(1) Atoms A and B must be connected by a path of maximum electron density (MED path). The existence of such a path implies a (3,–1) saddle point **r**_b of the electron density distribution ρ(**r**), as well as a zero-flux between atoms A and B (necessary condition).

(2) The local energy density *H*(**r**_b) has to be stabilizing, i.e. it must be smaller than zero (sufficient condition).

All calculations were performed with the ab initio program packages COLOGNE94⁴⁷ and GAUSSIAN92.⁴⁸ The IGLO method by Kutzelnigg and Schindler³⁹ and the PISA continuum model by Tomasi and co-workers³⁷ are implemented in COLOGNE94, where in the case of the IGLO method a direct version developed by Olsson and Cremer⁴⁹ was used to handle IGLO calculations with as much as 460 basis functions.

Acknowledgment. This work was supported by the Swedish Natural Science Council (NFR). Ab initio calculations were done on the Cray YMP/464 of the Nationellt Superdatorcentrum (NCS), Linköping, Sweden, as well as on the Silicon Graphics Power Challenge of MEDNET Computer Laboratory, Göteborg University, Sweden. D. Cremer and C.-H. Ottosson thank both the NSC and MEDNET for a generous allotment of computer time.

Supporting Information Available: Calculated energies and Cartesian coordinates of **1–18** (17 pages). Ordering information is given on any current masthead page.

JA9542956

(43)) Dauben, H. J.; Honnen, L. R.; Harmon, H. K. *J. Org. Chem.* **1960**, *25*, 1442.

(44)) (a) Chein, J. C. W.; Tsai, W. M.; Rausch, M. D. *J. Am. Chem. Soc.* **1991**, *113*, 8570. (b) Massay, A. G.; Park, A. J. *Organometallic Synthesis*; King, B. B., Eisch, J. J., Eds.; Elsevier: New York, 1986; Vol. 3, p 461. (c) Massay, A. G.; Park, A. J. *J. Organomet. Chem.* **1964**, *2*, 245.

(45)) Hariharan, P. C.; Pople, J. A. *Theor. Chim. Acta* **1973**, *28*, 213.

(46)) Ottosson, C.-H.; Cremer, D. To be published.

(47)) Gauss, J.; Kraka, E.; Reichel, F.; Olsson, L.; He, Z.; Konkoli, Z.; Cremer, D. *COLOGNE94*; University of Göteborg, Sweden, 1994.

(48)) Frisch, M. J.; Head-Gordon, M.; Trucks, G. W.; Foresman, J. B.; Schlegel, H. B.; Raghavachari, K.; Robb, M. A.; Binkley, J. S.; Gonzalez, C.; Defrees, D. J.; Fox, D. J.; Whiteside, R. A.; Seeger, R.; Melius, C. F.; Baker, J.; Martin, R. L.; Kahn, L. R.; Stewart, J. J. P.; Topiol, S.; Pople, J. A., *Gaussian 92*, Gaussian Inc.: Pittsburgh, PA, 1992.

(49)) Olsson, L.; Cremer, D. To be published.